

University of Southern Queensland
Faculty of Engineering and Surveying

**Ultimate Strength of Steel-Concrete Composite Beams
under Combined Bending and Torsion**

A dissertation submitted by

Mr. Matthew Neil Kronk

in fulfillment of the requirements of

Courses ENG4111 and 4112 Research Project

towards the degree of

Bachelor of Engineering (Civil)

Submitted: November, 2006

ULTIMATE STRENGTH OF STEEL-CONCRETE COMPOSITE BEAMS UNDER COMBINED BENDING AND TORSION

Sponsorship: The University of Southern Queensland



Matthew KRONK

Degree: Bachelor of Engineering, Civil

Supervisor: Dr. Qing Quan (Stephen)
Liang

1. INTRODUCTION

This dissertation seeks to further understand the combined effects of flexure and torsion on composite steel-concrete beams, beams often used in construction today. This will be done using the finite element analysis method, eliminating the need for high-cost, laboratory work.

2. BACKGROUND

Steel-concrete composite beams consist of a Universal Beam with a concrete slab lying on the upper flange of the Universal Beam. Composite action is achieved through a series of steel studs, which are welded to the upper flange of the steel beam, which are concreted within the concrete slab up to the middle layer. This connection is referred to as 'shear connection' and the number of steel studs used determines if full or partial shear connection exists.

Under combined torsion and flexure, there is very little information regarding to the ultimate loads of steel-concrete composite beams. In the late 70's and early 80's, a series of experiments was conducted in order to investigate the combined effect of flexure and torsion by R.K. Singh, S.K. Mallick (1977), B. Ghosh, S.K. Mallick (1979) and M. Basu Ray, S.K. Mallick (1980).

3. OBJECTIVES

This project aims to investigate the ultimate load behaviour of steel-concrete composite beams under the combined actions of bending and torsion using the finite element analysis program ABAQUS.

The results obtained will then be used to develop design formulas for the design of composite beams under bending and torsion.

4. METHODOLOGY

For the modelling of a non-linear steel-concrete composite beam, research into existing experiments needed to be made in order to verify the developed model.

The model developed was 3-dimensional to help stimulate geometric and material non-linear behaviour. The steel beam was modelled using shell elements, as was the concrete slab. The stud shear connectors were modelled using both beam and truss elements.

The model is then verified for accuracy before the generation of torque / moment interaction diagrams to display behaviour and for the derivation of design formulas relating to the ultimate torque and moment capacity of the member.

5. CONCLUSION

After the model was successfully verified, obtaining an ultimate strength within 10% of that achieved in the researched experiment, the model was tested under loading conditions of flexure and torsion.

The results obtained were not deemed to be suitable for the development of a moment/torque interaction equation due to the unusual behaviour observed.

6. ACKNOWLEDGEMENTS

I would like to thank my supervisor, Stephen Liang for his invaluable assistance during this project

University of Southern Queensland

Faculty of Engineering and Surveying

**ENG4111 Research Project Part 1 &
ENG4112 Research Project Part 2**

Limitations of Use

The Council of the University of Southern Queensland, its Faculty of Engineering and Surveying, and the staff of the University of Southern Queensland, do not accept any responsibility for the truth, accuracy or completeness of material contained within or associated with this dissertation.

Persons using all or any part of this material do so at their own risk, and not at the risk of the Council of the University of Southern Queensland, its Faculty of Engineering and Surveying or the staff of the University of Southern Queensland.

This dissertation reports an educational exercise and has no purpose or validity beyond this exercise. The sole purpose of the course pair entitled "Research Project" is to contribute to the overall education within the student's chosen degree program. This document, the associated hardware, software, drawings, and other material set out in the associated appendices should not be used for any other purpose: if they are so used, it is entirely at the risk of the user.



Professor R Smith

Dean

Faculty of Engineering and Surveying

CERTIFICATION

I certify that the ideas, designs and experimental work, results, analysis and conclusions set out in this dissertation are entirely my own efforts, except where otherwise indicated and acknowledged.

I further certify that the work is original and has not been previously submitted for assessment in any other course or institution, except where specifically stated.

Matthew Neil Kronk

Student Number: 0050011657



Signature

30/10/2006

Date

ACKNOWLEDGEMENTS

This project was carried out under the principle supervision of Dr. Qing Quan Liang and I would like to formally acknowledge the valuable assistance he provided me and for always having an open door.

Appreciation is also due to my friends and family for their encouragement and support provided throughout the year.

Table of Contents

Title Page.....	i
Abstract	ii
Limitations of Use	iii
Candidates Certification	iv
Acknowledgements	v
List of Figures	4
List of Tables.....	6
Chapter 1. Introduction	7
1.1 General	7
1.2 Background Information	10
1.2.1 Singh & Mallick (1977)	10
1.2.2 Ghosh & Mallick (1979)	13
1.2.3 Basu Ray & Mallick (1980)	14
1.3 Aims	16
1.4 Layout of this Dissertation	17
Chapter 2. Literature Review	19
2.1 Introduction	19
2.2 Nonlinear Analysis of Composite Beams.....	19
2.3 Experiments on Steel-Concrete Composite Beams.....	26
2.4 Composite Beams under Combined Bending and Shear.....	28
2.5 Conclusions	31
Chapter 3. Methodology	32
3.1 Introduction	32

3.2 Information Gathering	32
3.3 Finite Element Analysis	33
3.4 Model Validation.....	35
3.5 Moment-Torque Interaction Curves	36
3.6 Formula Development.....	36
3.7 Conclusions	37
Chapter 4. Finite Element Analysis	38
4.1 Introduction	38
4.2 The Finite Element Model.....	38
4.2.1 Concrete Slab	40
4.2.2 Steel Beam.....	40
4.2.3 Shear Connectors.....	40
4.2.4 Solution Method.....	41
4.3 Stress-Strain Curves for Steels	41
4.3.1 Steel Beam.....	42
4.3.2 Reinforcing Bars.....	43
4.3.3 Shear Connectors.....	44
4.4 Stress-Strain Curves for Concrete	44
4.4.1 Concrete in Compression	44
4.4.2 Concrete in Tension.....	46
4.5 Shear Retention	47
4.6 Conclusions	48
Chapter 5. Results & Discussion	50
5.1 Introduction	50

5.2 Model Validation.....	50
5.3 Moment-Torque Interaction	54
5.3.1 Boundary Conditions.....	55
5.3.2 Load-Deflection Curves	56
5.3.3 Moment-Torque Curves	59
5.3.4 Model Behaviour.....	61
5.4 Model Inadequacies.....	65
5.4.1 Rebar Layers.....	65
5.4.2 Material Properties and Modelling Techniques	66
5.5 Conclusions	66
Chapter 6. Conclusions	67
6.1 Summary.....	67
6.2 Further Research.....	68
Appendices	70
Appendix A, Project Specification	70
Appendix B, Load/Deflection Tables.....	72
References	83

List of Figures

Number	Title	Page
1.1	Steel-concrete Composite Beams	9
1.2	Loading Scheme	12
1.3	Ultimate moment-torque Interaction Diagram	12
1.4	Ultimate Strength Interaction Diagram	14
1.5	Ultimate Strength Interaction Diagram	15
3.1	Eccentric Load, Cross-section	34
3.2	Eccentric Load, Side View	35
4.1	Model Mesh	39
4.2	Cross-section of Composite Beam	39
4.3	Stress-Strain Curve, Steel	43
4.4	Stress-Strain Curve for Concrete	45
4.5	Stress-Strain Curve for Concrete in Tension	47
5.1	Comparison of Load/Deflection Results	53
5.2	Steel-Concrete Composite Beam under Pure Flexure	53
5.3	Simply Supported Composite Beam	55
5.4	Adopted Boundary Conditions for the Composite Beam	56
5.5	Load/Deflection Curve 1	57
5.6	Load/Deflection Curve 2	57
5.7	Load/Deflection Curve 3	58
5.8	Load/Deflection Curve 4	58
5.9	Load/Deflection Curve 5	58
5.10	Initial Moment/Torque Diagram	60

Number	Title	Page
5.11	Moment/Torque Diagram	61
5.12	Steel-Concrete Composite Beam under 120mm eccentric load	62
5.13	Steel-Concrete Composite Beam under 360mm eccentric load	62
5.14	Steel-Concrete Composite Beam under 400mm eccentric load	63
5.15	Cantilever Arrangement	64
6.1	Suggested Loading Scheme	68
6.2	Alternative Loading Scheme	69

List of Tables

Number	Title	Page
4.1	Material Properties Summary	48
5.1	Load/Deflection Data	51

Chapter 1. Introduction

1.1 General

Throughout the history of mankind, man has used and has experimented with numerous types of building materials. From the use of timbers, to sandstone bricks, man has sort to use many different sorts of materials to address issues such as strength, availability, cost and aesthetics. Today, the same issues apply.

Back in the days when stone was still a commonly used material, architects and engineers of the time were able to overcome the materials tensional limitations. Through the use of arches, most forces within a structure were effectively transformed into predominately compressive ones, allowing the structure to work to the materials advantage. This use of arches can be seen in Roman structures that still stand around the world today. This example not only teaches us how early architects and engineers were able to extend their current building “repertoire”, but it is also an example of how human ingenuity was able to solve a problem, was able to recognise how a material acts and works, and thus, design to exploit those properties.

Concrete is a modern day example. Today, it is one of the most widely used construction materials in the world, thanks in due to its mouldable shape, compressive strength and its economic attributes. But it really came into its own when concrete was started to be used as a composite structure. With internal steel reinforcement, the tensional limitations of concrete were able to be overcome, whilst maintaining its mouldable, economic properties. This discovery allowed concrete to become one of the most used materials in modern construction. This is

another example of overcoming a problem, of recognising a materials weakness and thus accommodating for it. Through composite action, concrete was enabled to be used in much broader scenarios.

What both these examples show is that through investigation of material behaviour, man has been able to extend the applications of that particular material.

Steel-concrete composite beams have been widely used in building and bridge construction. A composite beam is constructed by casting a reinforced concrete slab on the top of a steel beam. Composite action between the steel and the concrete is achieved by means of mechanical connectors. These connectors are generally dubbed as 'shear connectors'. They are typically connected by welding to the top flange of a steel beam and cast within the concrete slab. It is only through this connection that composite action is achieved, without these connectors, the concrete and the slab act independently and analysis is relatively simple. Shear connection significantly increases the strength and stiffness performance of composite beams. The amount of connectors provided designates what the composite beams shear connection is. A composite beam can be considered to have full shear connection or partial shear connection, proportional to the amount of shear connections. Shear connectors, according to AS 2327.1, can take the form of either headed studs, channels or high strength structural bolts. Similarly, the steel beam in a composite beam can take various shapes, as per AS 2327.1. The design code states that the steel must be structural steel, located below the concrete slab but connected, and must be symmetrical about its vertical axis. Figure 1.1 shows alternate beam types used in composite construction.

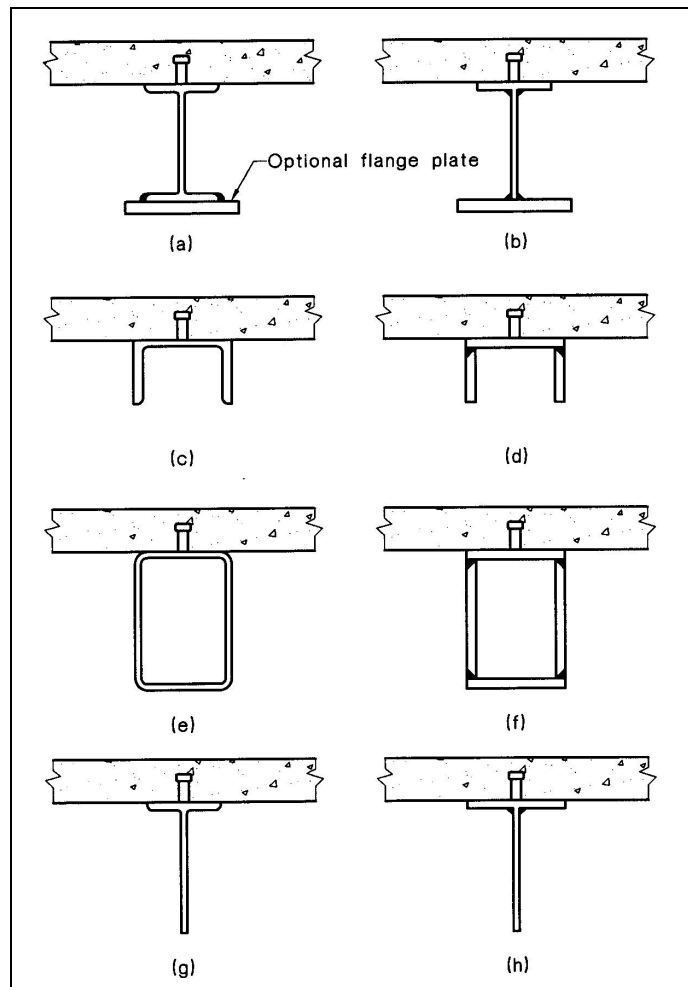


Figure 1.1 Steel-concrete composite beams

(Source: AS 2327.1 – 2003, p7)

AS2327.1 does not provide design rules for the design of composite beams under combined bending and torsion. This project seeks to investigate the behaviour of steel-concrete composite beams under the combined actions of bending and torsion. It is expected that this research will provide a better understanding of the behaviour of composite beams under combined flexure and

torsion and the proposed design formulas in this research project will be suitable for inclusion in AS2327.1 for the design of composite beams.

1.2 Background Information

Very little work on composite beams under combined flexure and torsion has been done. Singh and Mallick (1977) conducted experiments on steel-concrete composite beams subjected to torsion and combined flexure and torsion. In this paper, the authors also recognise the lack of work done in this area. Mallick and Ghosh (1979) studied the strength of steel-concrete composite beams under combined flexure and torsion. The interaction strength of composite beams under combined flexure and torsion was investigated by Ray and Mallick (1980). Since then, there has been very little research work conducted on this topic. The following sections summarise the results of the above papers.

1.2.1 Singh & Mallick (1977)

Singh and Mallick conducted ten experiments on composite beams with eight specimens. Two of the beams were retested. Four beams were tested under pure torsion and these beams were designated T-1, T-2 and so forth. The other four beams were tested under the combination of flexure and torsion and were designated FT-1, FT-2 and so forth. The loading patterns of these beams can be seen in figure 1.2.

In the paper, they presented a formula for determining the ultimate torsional strength of a composite beam. The formula presented was:

(1.1)

$$T_u = T_{cu} + T_r + T_j$$

where T_u was the ultimate torsional strength, T_{cu} was the contribution by the concrete, T_{tr} is the contribution of the reinforcement and T_j is the contribution from the joist. In the paper, two methods of calculating the contribution of concrete were presented. They came from Hsu (1968) and Colville (1972, 1973). In the experiments, the authors found that using Hsu's expression came to an ultimate torsional strength that was 7% less than the test results. Hsu's formula is as follows:

$$T_{cu} = \sqrt[3]{14.3x^5 y f_{cy}} \text{ in FPS units} \quad (1.2)$$

Hsu also presented the following expression for calculating the contribution from the reinforcement:

$$T_{tr} = 1.2x_1 y_1 \frac{A_s f_{sy}}{s} \text{ in FPS units} \quad (1.3)$$

The results interestingly showed that some beams under both flexure and torsion, were able to withstand a higher ultimate moment than that given by theory. It is thought that strength was added through combined action. The following interaction diagram of T/T_u and M/M_u was then developed in an attempt to visually represent this relationship (see figure 1.3).

In conclusion, they said that the shear connection principles outlined by Colville was satisfactory and that the formula presented above provides a reasonably close estimate of the torsional capacity. They also noted an increase in torsional capacity in the presence of flexure and vice versa.

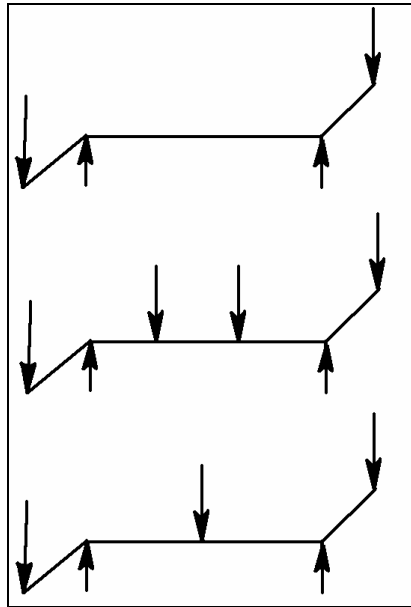


Figure 1.2 (dimensions neglected)

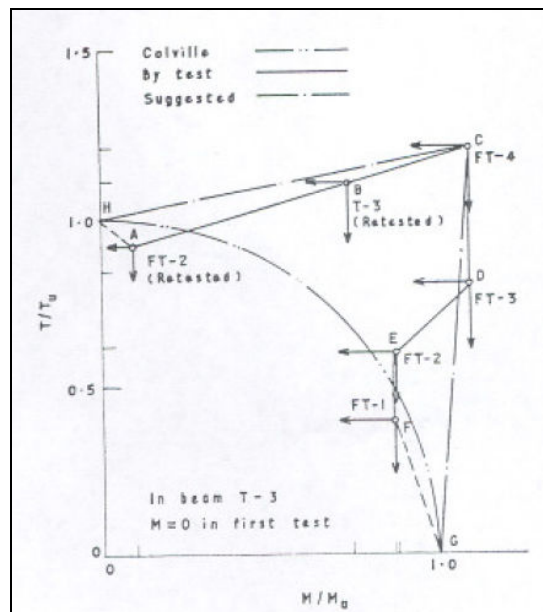


Figure 1.3 Ultimate moment-torque interaction diagram

(Source: R.K. Singh & S.K. Mallick, 1977, Indian Concrete Journal, p29)

1.2.2 Ghosh & Mallick (1979)

Ghosh and Mallick conducted experiments on six composite beams. The loading configurations were similar to those seen in figure 1.2. Five beams were tested under combined flexure and torsion and one beam was tested under pure torsion. This paper was intended to be a continuation of the previous paper by Singh (see section 1.1.1).

Strength in torsion was taken as:

$$T_u = T_c + T_s + (\leq T_j) \quad (1.4)$$

where T_j is the strength contributed by the joist, which is negligible compared to the contribution by the concrete. The contribution by the concrete was taken as:

$$T_c = 14.3x^{\frac{5}{3}}(f_{cy})^{\frac{1}{3}} \text{ in FPS units} \quad (1.5)$$

And the contribution by reinforcement as:

$$T_s = \alpha x_1 y_1 \frac{A_s f_{sy}}{s} \quad (1.6)$$

$$\alpha = 0.66m + 0.33 \frac{y_1}{x_1} \quad (1.7)$$

$$m = \frac{A_1 s}{A_s (x_1 + y_1)} \quad (1.8)$$

Subject to the limitations of $0.7 \leq m \leq 1.5$, and $\frac{y_1}{x_1} \leq 2.6$

They noted that the torsion formulation proposed by Singh leads to smaller values.

The produced another T/T_u and M/M_u diagram to represent the relationship. This diagram can be seen in figure 1.4.

The authors found it difficult to draw any conclusions on the behaviour of composite beams under flexure and torsion. They do however consider that the loading history of the beams may alter their general behaviour.

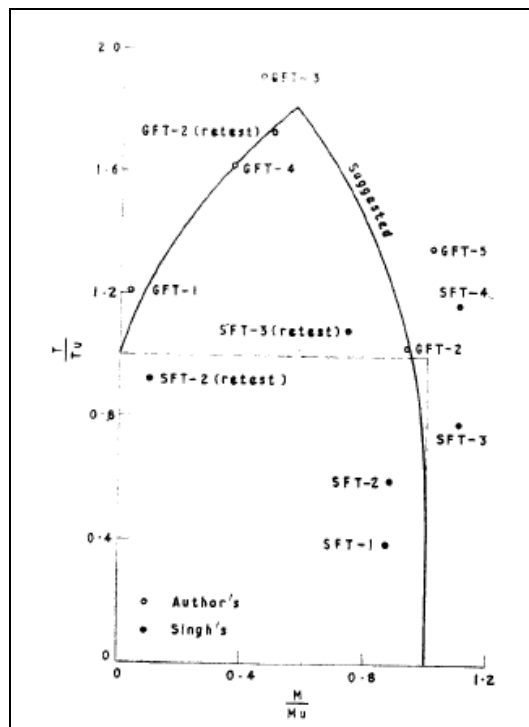


Figure 1.4 Ultimate strength interaction diagram

(Source: Ghosh, B. & Mallick S.K. 1979, Indian Concrete Journal, p52)

1.2.3 Basu Ray & Mallick (1980)

Basu Ray and Mallick continued on from the previous work of Singh and Ghosh. They noted that in Singh and Ghosh's experiments, they did not maintain a fixed flexure torsion ratio. The objective of Basu Ray and Mallick's tests was to observe the effects of maintaining a fixed ratio.

The experiment consisted of the testing of seven beams. One composite beam was under pure torsion, one sole concrete slab was under pure torsion and the remaining composite beams were under combined loading.

Again for the theoretical estimation of ultimate torsional load, the authors used the formula presented by Hsu, as in the previous study.

The T/T_u and M/M_u curve formulated can be seen in figure 1.5. From the experiments, Basu Ray and Mallick noted that torsional capacity increases with applied moment up to a certain point. This is an induced compressive force is applied to the top of the member in the presence of flexure. In conclusion, Basu Ray and Mallick said that the loading history, in this case the loading of flexure and torsion to a fixed ratio, doesn't have an appreciable effect on the behaviour of composite sections, under torsion and flexure.

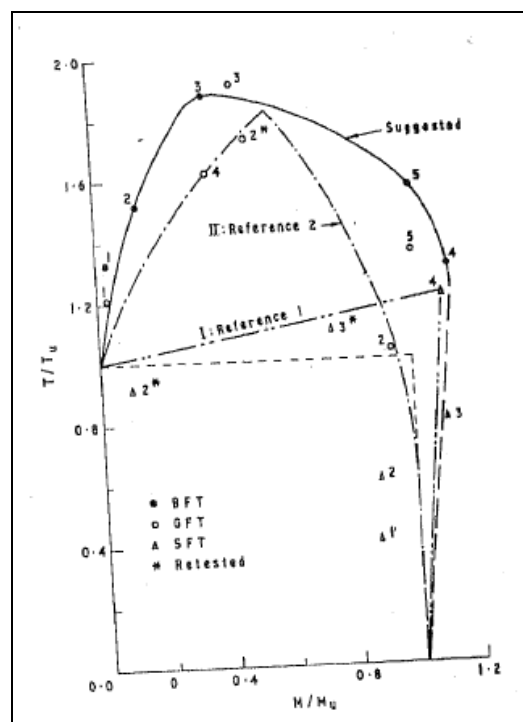


Figure 1.5 Ultimate strength interaction diagram

(Source: Basu Ray, M. & Mallick, S.K. 1980, Indian Concrete Journal, p83)

1.3 Aims

This project aims to investigate the ultimate load behaviour of steel-concrete composite beams, with full shear connection, under the combined actions of bending and torsion using the finite element analysis program ABAQUS (v6.5). The results obtained will then be used to develop design formulas for the design of composite beams under bending and torsion. It is envisioned that these aims be completed by meeting the following steps:

- Conduct a literature review on the experimental behaviour of composite beams and on the nonlinear finite element analysis of composite beams.
- Research into any experiments conducted on composite beams, particularly on similar loading conditions to obtain data for verification.
- Study the nonlinear finite element analysis method and develop a three-dimensional finite element model for the nonlinear analysis of composite beams under combined bending and torsion.
- Conduct nonlinear finite element analyses on composite beams with full shear connections under combined bending and torsion.
- Generate the ultimate moment-torque interaction diagram to display the interaction strengths of composite beams under combined actions.
- Based on the results obtained from the finite element analyses, develop design formulas that can be used for designing composite beams under similar loading conditions.

Should these steps be completed before schedule, the following step may be added:

- Modify the finite element models for composite beams with partial shear connections and conduct nonlinear analyses.

1.4 Layout of this Dissertation

Chapter 2 presents a literature review of experiments and new studies conducted on composite beams. It is broken down into three sections, “Nonlinear Analysis of Composite Beams”, “Experiments on Composite Beams” and “Composite Beams under Combined Bending and Shear”.

Chapter 3 presents the methodology of this project, detailing the method of analysis used and discussing the loading schemes, the model validation procedure and the expected results.

Chapter 4 discusses various subjects relating to the finite element analysis method. This section details the finite element model created and discusses the material properties and models utilised in the developed model

Chapter 5 presents the results obtained from the finite element analysis. It presents the results of the model validation test, a loading scheme inducing pure flexure, and presents the results obtained from loading schemes inducing flexure

and torsion. The slight modelling differences between the model validation phase and the moment-torques phase are discussed.

Also discussed are the limitations of the developed model and there effects on the estimated ultimate loads.

Chapter 6 summarises and concludes the current study and identifies areas of further research.

Chapter 2. Literature Review

2.1 Introduction

The aim of the literature review is to investigate the current level of the state of the art of the research topic. In the case of this project, the following review covers topics of experiments on steel-concrete composite beams, finite element analysis of composite beams and research into combined effects.

2.2 Nonlinear Analysis of Composite Beams

Thevendran et al. (1999) investigated ultimate load behaviour of curved composite beams. The authors created a three-dimensional finite element model, using ABAQUS, to predict the load-deflection behaviour of curved composite beams. They then compared the computed results with experimental results obtained by the authors in a previous study.

The concrete slab, in the finite element model, was modelled using four-node isoparametric thick shell elements with the coupling of bending and membrane stiffness. The concrete in compression was modelled as an elastic-plastic material with strain hardening. The uniaxial stress-strain curve was used for compressive concrete, which is expressed by

$$f_c = f' \left[\frac{2\varepsilon_c}{\varepsilon_0} - \left(\frac{\varepsilon_c}{\varepsilon_0} \right)^2 \right] \quad (2.1)$$

where f' is the cylinder compressive strength of concrete in MPa, ϵ_0 is the strain corresponding to the maximum compressive stress, taken as 0.002 and ϵ_{cu} is the strain at which concrete crushes, taken as 0.0038.

The stress-strain behaviour of concrete in tension was expressed by a bilinear curve, where stress increases linearly with strain up to the maximum tensile stress and then falls linearly back to zero stress with increasing strain. This constitutes a strain softening model. Steel was modelled as a strain hardening material in both compression and tension. They also adopted a shear retention model which assumes that the shear stiffness of open cracks reduces linearly to zero as the crack widens.

The results obtained by Thevendran et al. (1999) show that their adopted finite element model could be used for the prediction of ultimate strength. The maximum deviation obtained was 14%. The model did however have trouble predicting crack loads, with deviations lying between -29% and 23%.

Hirst and Yeo (1980) developed a method of creating 2-dimensional finite element models to represent composite beam behaviour using standard elements. They demonstrated that standard finite element programs could be used to analyse the elastic range and the full load deflection of composite beams and thus, that the proposed method could therefore be available to use by the design engineer in the office.

Hirst and Yeo (1980) presented a method of modelling slip interaction without the use of special slip elements. These elements are then given appropriate properties to behave correctly.

The models developed were then tested and compared to existing published results. They analysed a concrete rectangular beam and a composite steel-concrete beam in the elastic range.

A non-linear analysis was also undertaken to predict the load-deflection curves of composite beams. The results obtained were then compared to experimental results obtained from Yam and Chapman (1968). Comparisons showed that the model predicts values within 5% of those obtained from the mentioned experimental values. The model was then used with 75, 50 and 25% of the studs needed for full interaction. Hirst and Yeo (1980) then concluded that the method outlined can be used for the finite element analysis of composite beams.

Yam and Chapman conducted a series of numerical tests, accompanied by experimental tests, to investigate the inelastic behaviour of composite beams. This investigation arose out of shortcomings seen in The Code of Practice for Composite Construction (CP117, Part 1, Simple Beams in Buildings) as of 1968.

The numerical analysis employed was the predictor-corrector method of step by step numerical integration. The analysis ran under a couple of assumptions. These assumptions included: linear distribution of strain over the depth of the slab and the beam, that the shear connection, over the length of the beam, acts as a continuous medium, the stress/strain curves for steel are the same in tension and compression and that the concrete and the steel have equal curvature at all points along the beam and that uplift forces are entirely resisted by the shear connectors without separation. These assumptions were proved to be adequate, as the numerical analysis developed, yielded results that satisfactorily correlated with test results.

The experiments produced a wide variety of results. A number of the beams were designed with shear connection complying with Part 1 of CP 117. This was done to test the validity of the design codes. It was found that for a point load located mid-span, the ultimate load of a standard beam was found to be 6% lower than the value obtained through the CP 117 procedure. Low rigidity shear connections were also found to result in point load ultimate moments to fall 10% short of the value obtained by CP 117.

In all relevant results, strain hardening resulted in ultimate moments 17-33% higher than those obtained through CP 117. Strain hardening does however increase the likelihood of shear failure.

Shear connection was also investigated and it was found that a 10% reduction in the number of shear connectors resulted in shear failure for uniformly distributed beams, whereas beams with point loads required a 65% reduction before shear failure.

Yam and Chapman came to the conclusion that CP 117 provides adequate methods for the calculation of ultimate moment, and for the distribution of shear connection.

Razaqpur and Nofal developed a new method of representing stud shear connectors in finite element analysis. Previous to this paper, stud connectors were represented as rigid or elastic springs, a smeared layer, or simply it is assumed that there is full interaction. The element proposed by Razaqpur and Nofal is a three dimensional bar with two end nodes and three translational degrees of freedom at either end. The elemental formulation came forth from the empirical equation of Yam and Chapman (1968).

The model was compared with experimental results from Yam and Chapman (1968) with favourable outcomes. The experimental and the finite element models closely compared, with major deviations being brought down to normal experimental abnormalities. The finite element models were only partially modelled, due to symmetry, and it is in this symmetry that the differences are noted. In general, the finite element model responded in a stiffer manner, though the ultimate load was accurately predicted.

In conclusion, Razaqpur and Nofal reported that the three dimensional bar element was both simple and effective in finite element analysis, though they did conclude that further experimentation should be done in more general loading conditions, i.e. torsion and two dimensional shear.

Razaqpur and Nofal developed a finite element program to account for the nonlinear behaviour of steel-concrete structures. This program was dubbed NONLACS, for NONLinear Analysis of Concrete and Steel.

Concrete in the program was modelled in two parts. In compression, concrete was modelled according to the equation proposed by Saenz (1964) and in tension concrete was modelled following the Smith-Young model. Steel was modelled as a strain hardening material, both in tension and compression.

The shear connectors were modelled using bar elements, utilising an empirical equation, developed by Yam and Chapman (1968), to account for the shear force/slip relationship. This same method of shear connection modelling was used and described by the authors in their previous paper (1989).

The developed program was then used to compare computed results with published experimental results of differing origin.

The first validation test was compared with results obtained by the developers of the empirical shear force/slip equation, Yam and Chapman (1968, 1972). The program resulted in an ultimate shear load which was within 1.20% of the experimental result. The following test was with results obtained from Hamada and Longworth (1976), to test the robustness and the accuracy of both the program and the shear force/slip equation. Maximum differences in this test were less than 3%. The final analysis was of a multi-girder bridge, which was tested to destruction by investigators from the University of Tennessee. The results obtained showed maximum differences of about 4%. The examples showed that their program can be considered reliable for the analysis of inelastic response, load distribution and ultimate strength of complex multi-girder and multi-span bridges, though the authors recognised that the program is currently incapable of accurate results when failure is initiated by large deformations and/or buckling.

Sebastian and McConnel (2000) developed a finite element program with the ability to model steel-concrete composite beams with profiled steel sheeting. The program developed was then tested against a series of experimental tests to check the validity of the program code.

Concrete was modelled nonlinearly as an elastic isotropic material, as proposed by Cedolin (1977), and the formulated stress-strain relationships follow Cedolin's proposal. Post cracked or crushed concrete was modelled as an orthotropic material. This modelling required new constitutive equations, which are discussed by the authors. Steel was modelled as an elasto-plastic material with strain hardening. For verification, the program was used to analyse a reinforced concrete slab tested by McNeice, a continuous composite beam tested by

Teraskiewicz, a model composite bridge tested by Newmark et al and a composite space truss bridge tested by Sebastian and McConnel. The continuous composite beam that was analysed against that tested by Teraskiewicz, was modelled with the shear force/slip empirical equation proposed by Yam and Chapman (1972).

The Finite Element program developed showed to be a very robust tool for predicting the failure behaviour of steel-concrete composite structures. The program also showed to be accurate in predicting internal deformations, shear connector actions and crack patterns. The program's capabilities could be extended to account for in-depth shear and to handle nonlinear geometric effects.

Baskar, Shanmugam and Thevendran (2002) conducted a series of finite element analyses on steel-concrete composite plate girders. Their analyses used negative bending and the results obtained were compared to experimental results obtained from Allison et al. (1982).

A number of finite element models were developed in an attempt to find the most appropriate method. The changes between the models differ in the modelling of concrete. Because composite plate girders reach failure after the tensional failure of concrete, the Baskar, Shanmugam and Thevendran presented several different models.

Concrete was modelled as a linear elastic plastic strain hardening material. In the model, the uniaxial compressive stress-strain curve is assumed to be linear up to $0.3f_c$ and then follows the expression suggested by Carreira and Chu (1985). In tension, concrete was modelled to be linear up to a maximum tensional stress, followed by a linear decrease in stress with strain, a strain softening model. Steel was modelled as a strain hardening material.

The deck slab when modelled using 3D solid elements, used different material models, such as: CONCRETE MODEL, CAST IRON MODEL and the ELASTIC-PLASTIC MODEL. Of the models, the cast iron model was found to predict the ultimate load closer to the experimental value.

The deck slab was also modelled using thick shell elements. This method was found to be the most effective. Although all models predicted the ultimate load to a reasonable accuracy, it is the thick shell element model that can be used to extend the analysis to failure. The model was found to be the best for predicting the behaviour of a composite plate girder in both the elastic and plastic regions.

2.3 Experiments on Steel-Concrete Composite Beams

Chapman and Balakrishnan (1964) conducted a series of experiments on simply-supported steel-concrete composite beams. They investigated the effects of shear connectors on the ultimate strength of composite beams, as well as slip. In all, they conducted 17 live tests, with each beam having a different shear connection or loading pattern. They came to various conclusions about stud action, slip and the affect they have on attaining perfect composite action between the concrete and the steel section. Their results showed that current design methods were appropriate, in that flexural failure occurred before shear connection failure. They also suggested that shear connectors need to be properly anchored within the compression zone of the slab and that studs with smaller diameters are slightly more efficient for a given cross-sectional area.

Ansourian (1981) carried out experiments on six continuous composite beams all 9m long and having a compact steel section. The major variables were

loading configuration, slab width and geometry of steel joist. Ansourian had differing ductility parameter values. Ansourian was particularly interested in investigating hogging hinges (beams 3-6) and beams 1-2 were to provide more insight into problems of sagging rotation.

Ansourian proposed that beams with a ductility parameter χ greater than 1.4 could be designed using simple plastic theory.

Experiments showed that an increase in slab width increased capacity as well as ductility parameter χ (beams 1 and 2) and that greater sagging rotation and strain-hardening capacity increase with slab width.

Ansourian's results concluded that sections design with a ductility parameter χ greater than 1.4 can be designed according to simple plastic theory. The expression for ductility parameter χ is given in the paper.

Yam and Chapman (1968) conducted a series of experiments on continuous composite steel-concrete beams. Their analysis method was a numerical method, which was presented in an earlier paper by Yam and Chapman (1968). They had two simultaneous non-linear ordinary differential equations of the first order.

Different loading scenarios were analysed, including point loads and uniformly distributed loads.

They concluded that for symmetrical two-span continuous beams, with either symmetrical point loads or a uniformly distributed load, the simple plastic method can be used to calculate the collapse load. Their other conclusions gave advice to spacing of shear connectors with regard to sections of maximum

moment, and for the calculation of the position of maximum moment of uniformly distributed loads.

2.4 Composite Beams under Combined Bending and Shear

Baskar and Shanmugam (2003) conducted some experiments and finite element analysis on steel-concrete composite plate girders subject to the effects of combined shear and bending.

A number of experiments were conducted with varying depth to thickness ratios, flange dimensions, spans, moment/shear ratios and loading types. Both positive and negative bending was investigated.

The experiments showed that through composite action, the shear capacity of the web increased therefore increasing the capacity. This combined action effect was more pronounced in the beams subject to positive bending. The axial tension, induced by bending, stabilized the shear buckling behaviour of the web.

The authors came to the conclusion that composite action is more effective for girders with slender webs, as the percentage increase in capacity is more significant.

The finite element analysis conducted was able to predict the ultimate load and behaviour with reasonable accuracy, they did however have trouble with convergence post ultimate failure load.

Liang et al. (2005) conducted a series of finite element analyses to investigate the behaviour of composite beams combined bending and shear. The model developed was then validated by existing experimental results presented by Chapman and Balakrishnan (1964).

Doubly curved thick/thin shell elements were used to model the concrete slab, the web and the steel flanges. The shear connectors were modelled using 3D beam elements.

Concrete was modelled using the stress-strain relationship defined by Carreira and Chu (1985). In compression, concrete was assumed to behave linearly in the elastic region up to $0.4f_c$. In tension, it was assumed that tensile stress increases linearly with increases in tensional strain up to cracking, where it linearly decreases as the crack opens. The shear retention model was used was that suggested by Thevendran et al. (1999) and Liang et al. (2004). Steel was modelled as a strain hardening material with an assumption of 0.25 for the ultimate strain. This material property was applied to all steel members.

The model was validated by comparing results of a beam tested by Chapman and Balakrishnan (1964). The model predicted an ultimate load of 95.3% of the experimental load, which suggests that it is conservative.

Liang et al. found that with an increase in the moment/shear ratio, the ultimate load decreases. They also found that the concrete slab increases the maximum shear strength of the beam by 85%, through composite action, which is significant considering that design codes consider that the steel web resists the entire vertical shear.

The authors then present a design model for strength interaction, which mimics the numerical results well. They concluded that their model is a consistent and economical design procedure for the design of simply supported composite beams.

Liang et al. (2004) developed a 3D finite element model for predicting the behaviour of continuous steel-concrete composite beams under combined bending and shear.

Concrete was modelled as a four node doubly curved shell element with reduced integration. It was assumed to behave linearly up to $0.4f_c$ and then follow the expression presented by Carreira and Chu (1985). Concrete in tension was assumed to be a strain softening material. It was assumed that concrete tensile stress linearly reaches its maximum value and cracks, after which, the tensile stress linearly decreases to zero as the crack widens.

Steel was modelled as a four node doubly curved shell element. It was given a trilinear stress-strain curve, representing the nonlinear behaviour of strain hardening. Reinforcing bars were modelled as Rebar layers within the concrete slab.

The finite element model was tested for validation against an experiment conducted by Ansourian. The validation test yielded an ultimate load which was 97.2% of the experimental value, which lead to the conclusion that the model developed was both conservative and reliable.

The model was then used to test composite beams with various moment/shear ratios and shear connection values. The tests indicated that the concrete contributes a significant amount of shear strength to the ultimate shear strength of the composite beam and that shear strength generally increases with an increase in shear connection. With the obtained results, a series of design formulas were developed which defines the relationship between ultimate strength and shear strength, with proposals that take shear connection, stud pullout failure and

shear capacity of the steel web into account. The models were verified against existing experimental data obtained from Ansourian (1981) and were found to be accurate and economical and were therefore found to be suitable for inclusion in design codes.

2.5 Conclusions

The area of steel-concrete composite beams has had quite a good amount of work conducted on it over the years. Various studies have gone into investigating the effects of combined forces, shear connection, shear connectors, geometric effects, finite element analysis and modelling. In particular, various attempts have been made at modelling concrete, a very non-homogenous, nonlinear material in a finite element package. A mixture of empirical and theoretical equations has been developed for the analysis of composite beams.

The literature review, in particular, highlighted the need for further studies on the effects of combined torsion and flexure on composite beams, due to the small amount of information available.

Chapter 3. Methodology

3.1 Introduction

This project will investigate the following important aspects of composite steel-concrete beams under combined bending and torsion:

- Information gathering;
- Finite element analysis of composite beams under combined bending and torsion;
- Develop moment-torque interaction curves for composite beams;
- Finite element model validation; and
- Formula development.

These parts are presented and explained separately below in order of sequence.

3.2 Information Gathering

This section involved research to gather information relevant to this project. This included the material gathered and collated in the literature review above. The project however, as mentioned above, calls for validation and comparison of results with existing results. This meant that there was need to find existing, published information on composite beams under the combined effects of bending and torsion.

These results were found in three journal articles in particular, from the Indian Concrete Journal. A brief overview of the contents of these articles is provided in the section above, Background Information.

3.3 Finite Element Analysis

The finite element analysis method will be used to investigate the ultimate strength and behaviour of steel-concrete composite beams under combined bending and torsion. A three-dimensional finite element model will be developed to simulate the geometric and material nonlinear behaviour of composite beams under combined actions of bending and torsion. Shell elements will be employed to model the steel beam and concrete slabs. Stud shear connectors will be simulated using beam elements. Rebar Option in ABAQUS will be used in the finite element model to include the reinforcement in concrete slabs. The finite element model developed will be employed to analyse composite beams under combined bending and torsion. The model needs to be modelled to conform to pre-existing experimental data, for accurate comparison. Beyond the modelling stage there is a pre-validation stage and a post-validation stage (see section on validation). Pre-validation involves a finite element analysis of the model under a more simplistic loading case, e.g. simple bending. Beyond this initial analysis is post-validation where the model is put under the combined loads relevant to this project.

Bending moment and torque will be applied by eccentrically loading the point load applied to the developed composite beam model. This loading scheme will apply a moment and torque that is proportional to each other. Figure 3.1

displays, in cross-section, how an eccentric load applies torque acting around the length of the beam.

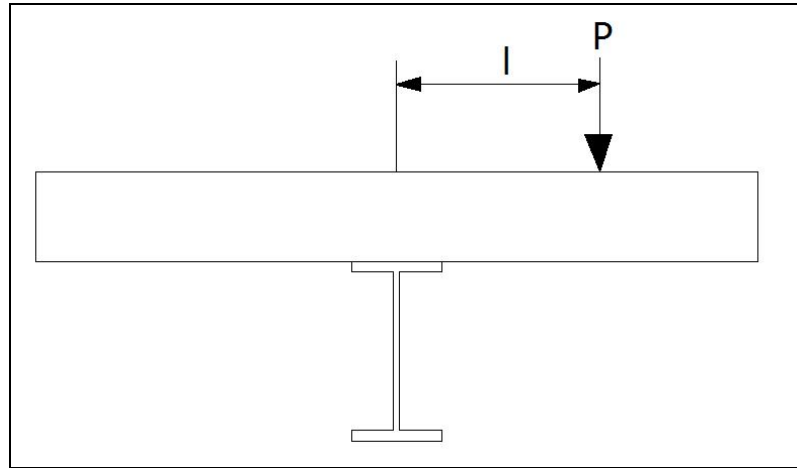


Figure 3.1 Eccentric load, Cross-section

Figure 3.1 displays the load, “P” and the eccentricity from the centre, “ l ”. The result is a moment or torque acting down the depth of the beam. That torque is calculated by:

$$T_u = P_u \times l \quad (3.1)$$

where, “ T_u ” is the ultimate torque, “ P_u ” is the ultimate applied load and “ l ” is the eccentric length.

The Ultimate moment is calculated in a similar fashion. Figure 3.2 depicts the loading case looking from the side.

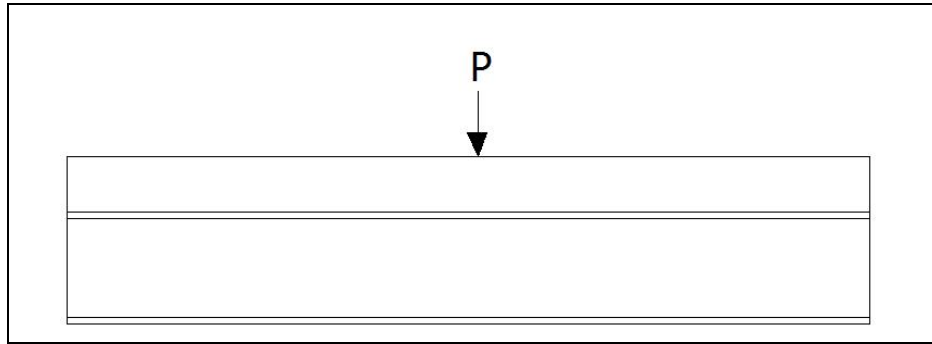


Figure 3.2 Eccentric load, Side view

The ultimate moment is given by:

$$M_u = \frac{P_u \times l}{4} \quad (3.2)$$

where, “ M_u ” is the ultimate moment, “ P_u ” is the ultimate point load and “ l ” is the overall length of the beam.

3.4 Model Validation

Existing experimental data will be used to validate the finite element models developed for composite beams under combined bending and torsion. The results obtained from the nonlinear finite element analysis will be compared with experiments on composite beams under bending and then under combined actions of bending and torsion. Validation is important to establish the reliability of the models performance, and ultimately, the results of the project itself.

3.5 Moment-Torque Interaction Curves

The finite element analyses on composite beams under various combinations of bending and torsion will be carried out in order to generate the ultimate moment-torque interaction diagrams. Curve analysis is done after post-validation finite element analyses. With the gathered data, obtained from the computer results, a series of curves can be drawn. The most important of these curves is the torque/moment interaction diagram. Examples of experimentally based torque/moment diagrams can be seen in Background Information. A curve will then be fitted to the diagram, in an effort to define the relationship between ultimate torque capacity and ultimate moment capacity.

3.6 Formula Development

This section leads on from the curve analysis. With the fitted curve, formulas pertaining to that curve are derived to form an expression which relates the moment capacity and torque capacity of steel-concrete composite beams. A lower bound torque/moment interaction expression has been suggested. It can be found in Singh and Mallick (1977). It is expressed as follows:

$$\left(\frac{M_F}{M_u}\right)^2 + \left(\frac{T_F}{T_u}\right)^2 = 1 \quad (3.3)$$

where: M_F is the failure moment, M_u is the theoretical ultimate moment, T_F is the failure torsion and T_u is the theoretical ultimate torsion.

The above interaction equation is too conservative. A design formula for predicting the ultimate strengths of composite beams under combined bending and torsion will be proposed in this research based on the results obtained from the nonlinear finite element analysis of composite beams. Analytical methods as presented by Liang et al. (2004, 2005) will be employed to develop the design formula.

3.7 Conclusions

This project involves both computational analysis and data analysis. The results' accuracy obtained from the methods outlined above, relies heavily on the accuracy and reliability of the results obtained from the computational analysis. Therefore, caution must be used in determining the reliability of any obtained results.

Chapter 4. Finite Element Analysis

4.1 Introduction

The Finite element method was used for the analysis of steel-concrete composite beams. Various load combinations had to be employed both for results and for model validation. The following sections detail the finite element model itself, as well as document the material properties employed in the hopes of achieving an accurate, reliable finite element model.

4.2 The Finite Element Model

The 3D finite element model developed accounts for material and geometric non-linear behaviour to study the effects of flexure and torsion on steel-concrete composite beams. Figure 4.1 displays the model mesh. The rectangular section on the top of the model represents the concrete slab, it was modelled with shell elements and measures 13 x 61 elements. The steel joist was also modelled using shell elements and measures 60 elements in length, with widths of 3 elements for the web and 2 elements for the flanges. The shear connectors were modelled using both beam and truss elements. The finite element package utilised was ABAQUS version 6.5.

The model composition can be seen in Figure 4.2, which displays the dimensions and overall layout of the composite beam.

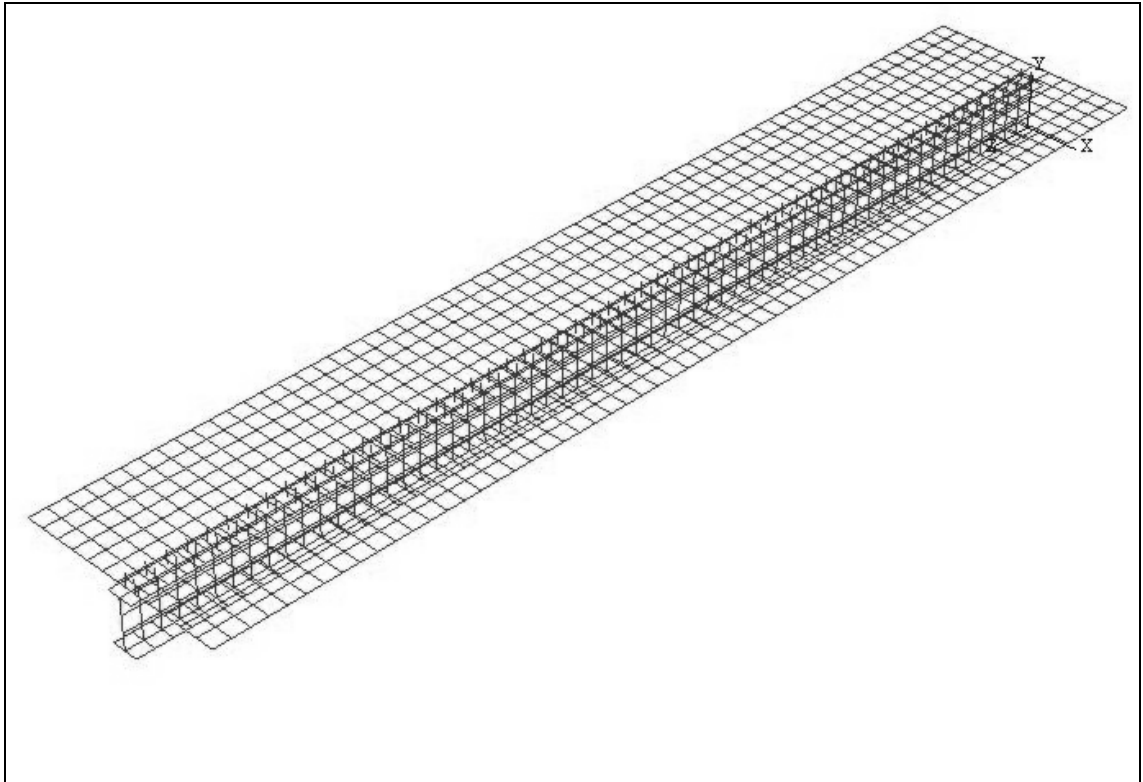


Figure 4.1 Model Mesh

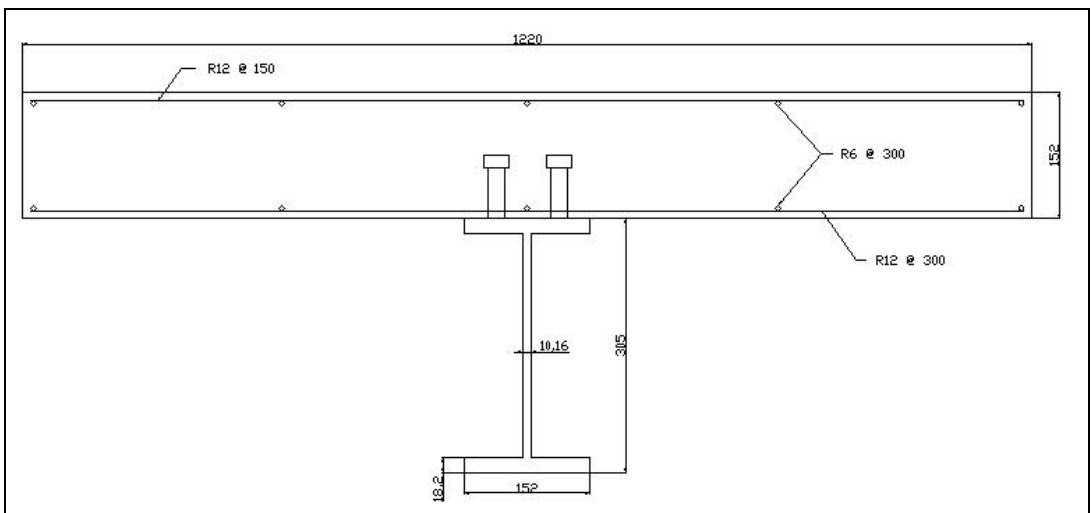


Figure 4.2 Cross Section of Composite Beam

4.2.1 Concrete Slab

The concrete slab was modelled using the element type S4R, which is a four node, doubly curved shell element with reduced integration. Five integration points were taken through the depth of the slab. The slab was given concrete properties that made account for the reinforcement. The reinforcement is included via rebar layers. For further information regarding concrete material modelling, refer to section, **4.4 Stress-Strain Curves for Concrete**.

The concrete slab was given a mesh density that resulted in the slab having elemental lengths of 61 elements (long) by 13 elements wide.

4.2.2 Steel Beam

The steel beam was modelled using four node, doubly curved shell elements with reduced integration, as with the concrete slab. Both the flanges and the web were analysed with five integration points throughout their respective thicknesses.

The steel beam was given a mesh density which resulted in the flange having 2X60 elements and the web with 3X60 elements.

4.2.3 Shear Connectors

Shear connectors were modelled using two elemental types. The first type of element used was B31, which is a two node linear beam. With this element type, a pair of studs was modelled and then given multiple instances within the model assembly. This elemental type is used for providing the shear and stiffness

of the actual shear connectors. The second element used was T3D2, which is a two node linear 3D truss. This element type was also used by creating a pair of studs, which was given multiple instances within the model assembly. The truss and beam elements are arranged to occupy the same space. The pin jointed truss elements are used to transfer direct stress from the concrete slab to the steel beam. In all cases, the shear connectors were assumed to connect from the upper steel flange to the inner centroid of the concrete slab. This method of shear connector modelling was proposed and used successfully by Liang et al. (2004, 2005).

4.2.4 Solution Method

The solution method adopted was the modified Riks method. The additional control, “analysis=discontinuous”, was used to help prevent the discontinuities present due to concrete cracking. The beam was monitored additionally for deflection at mid-span and the load application was applied automatically.

4.3 Stress-Strain Curves for Steels

The composite beam is constructed from several parts which combine to make the composite structure. Three of those parts are made of steel with varying material properties between them. These differing properties have to be specified

within ABAQUS to ensure that individual parts exhibit behaviour that is consistent with the material they are trying to mimic.

Material properties need to be specified for the steel beam itself, the concrete reinforcement or “reo”, and the shear connectors or “studs”. This means that property values need to be generated in order for the program to mimic the behaviour of the materials. With steel, modelling is fairly straightforward because it is homogenous and because there is little variation in strength, from member to member.

4.3.1 Steel Beam

The steel beam was modelled within ABAQUS as an isotropic material that exhibits both the elastic and plastic behaviour of steel as well as the non-linear effect of strain hardening. A typical Stress-Strain curve for steel displaying properties of strain hardening can be seen in figure 4.3.

The steel in this case, was modelled with a Young’s modulus of 205350 MPa and a Poisson’s ratio of 0.3. The yield strength was designated as 265 kN and the ultimate strength was set at 410 kN.

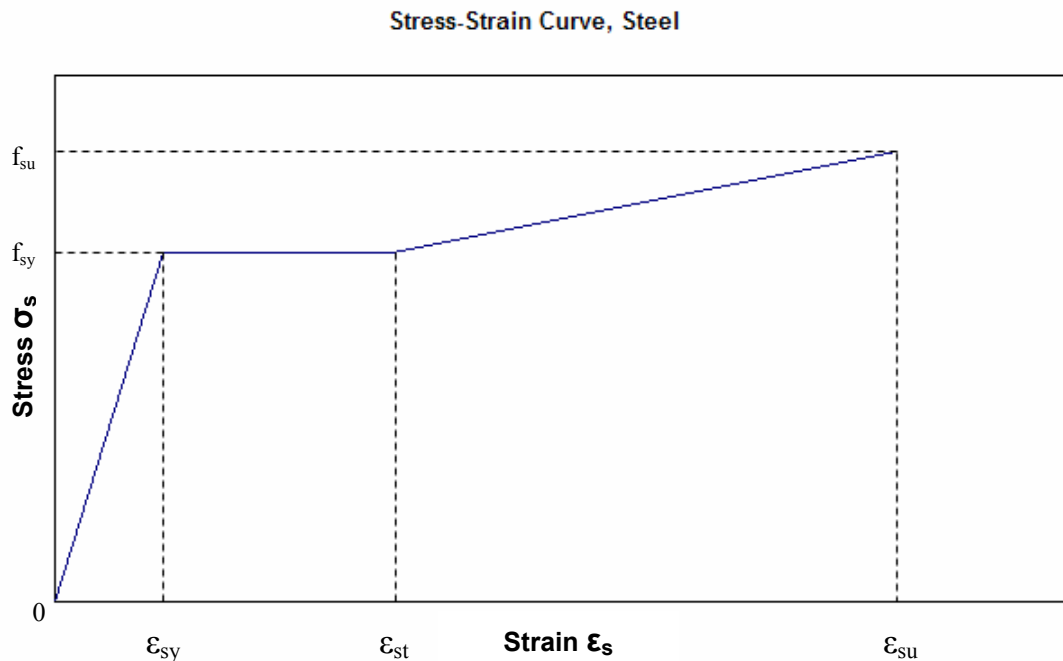


Figure 4.3 Stress-Strain Curve Steel

4.3.2 Reinforcing Bars

The reinforcing bars were modelled using the “rebar layer” option. Using this option, the reinforcing bars are not individually input by the user but are generated. When the reinforcing is generated, ABAQUS asks for material properties to apply to the rebar layer (For reinforcing layout details, see the previous section, 4.2 The Finite Element Model.).

The reinforcing was modelled as an isotropic material with elastic and plastic behaviour. The yield stress of the steel was 250 MPa, in Australia this is designated as “R-type” reinforcing. The Young’s modulus was designated as 200,000 MPa with a Poisson’s ratio of 0.3. The Stress-Strain curve for the reinforcing follows the same pattern as displayed in figure 4.3 above.

4.3.3 Shear Connectors

The shear connectors were modelled using the same tri-linear stress-strain relationship as presented in figure 4.3 above. They were given a yield strength of 410 kN and an ultimate strength of 580 kN.

4.4 Stress-Strain Curves for Concrete

Concrete is a lot more difficult to model in a finite element package. Numerous people have come up with different methods and formulae in an attempt to make a thorough algorithm to mimic the behaviour of concrete, both in compression and tension. Unlike steel, concrete does not have a homogenous makeup. Concrete itself is a composite structure. It consists of an aggregate material that is interlocked together and bound with cement. Aggregate interlock is complex and inconsistent, adding complexity to the theoretical modelling of concrete. Adding to the complexity is the difference that concrete curing or vibration makes to the strength of the concrete. Therefore, an adequate concrete model needs to be utilised to ensure that the required reliability is obtained.

4.4.1 Concrete in Compression

Concrete was modelled under the “Concrete smeared cracking” option, when creating a new material. As with the steels, a stress strain curve needs to be generated to define the compressive behaviour of concrete. The following figure, figure 4.4 displays the compressive strength of the concrete used in this model.

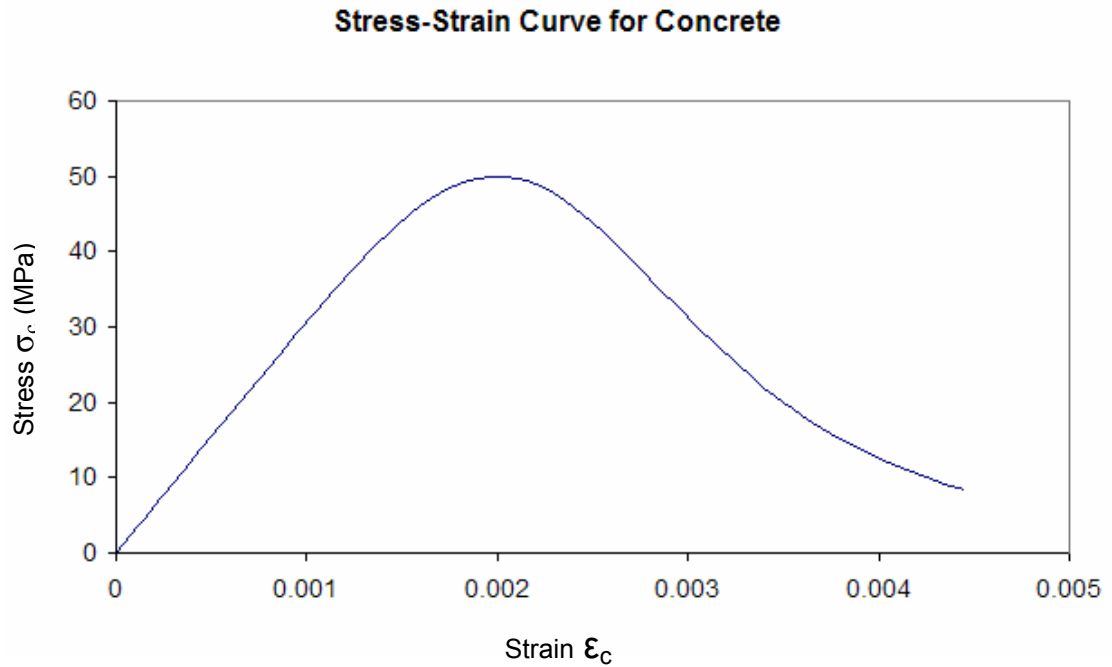


Figure 4.4 Stress-Strain Curve for Concrete

The above representation was calculated using the uniaxial compression relationship proposed by Carreira and Chu (1985), and used with success by Liang et al (2005). This relationship is expressed by:

$$\sigma_c = \frac{f'_c \gamma (\epsilon_c / \epsilon'_c)}{\gamma - 1 + (\epsilon_c / \epsilon'_c)^\gamma} \quad (4.1)$$

where: σ_c is the compressive stress, f'_c is the cylinder compressive strength of concrete, ϵ_c is the strain in concrete, ϵ'_c is the strain in the concrete corresponding to the value f'_c and γ is represents:

$$\gamma = \left| \frac{f'_c}{32.4} \right|^3 + 1.55 \quad (4.2)$$

In this case, the value of ε'_c was taken as 0.002. The behaviour up to $0.4f'_c$ was assumed to be linear elastic. Within ABAQUS, the failure ratio option was utilised. This allows the input of failure ratios for ultimate biaxial stress to ultimate uniaxial stress, as well as uniaxial tensile stress to the uniaxial compressive stress at failure. These values were taken as 1.16 and 0.0836 respectively. Within the elastic region, the Young's modulus was taken as 35,709 MPa and the Poisson's ratio was taken to be 0.15.

4.4.2 Concrete in Tension

Concrete in tension was modelled by using the tension stiffening model. This model assumes that as a crack opens, the direct stress linearly decreases to zero. A representation of the model used can be seen in figure 4.5.

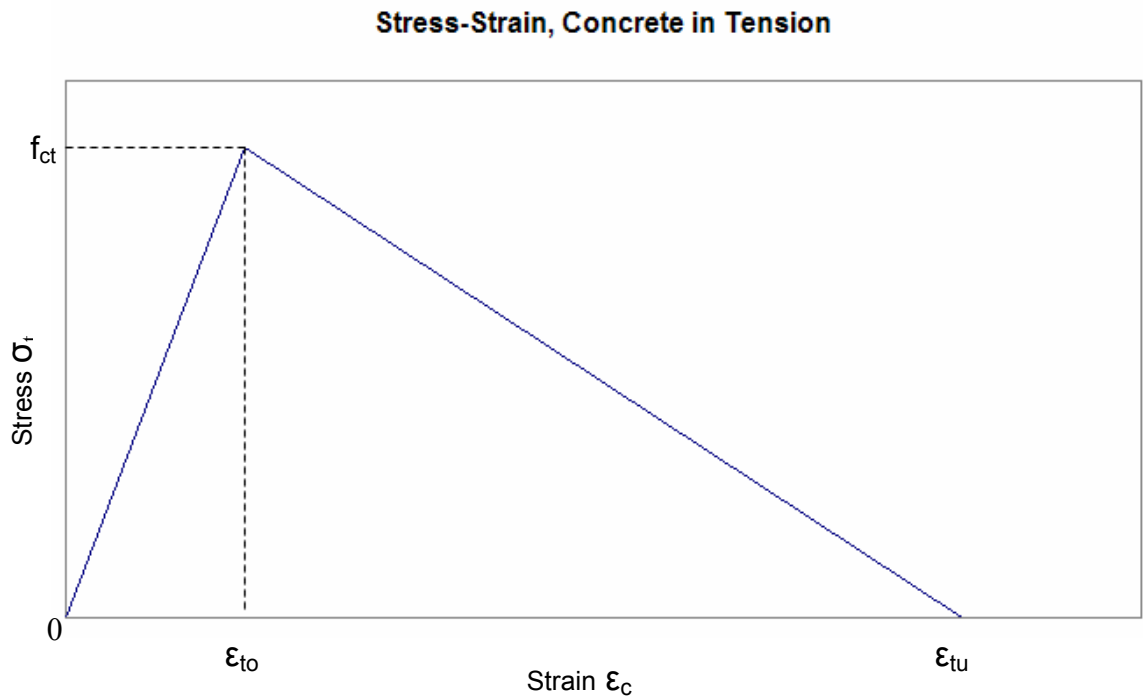


Figure 4.5 Stress-Strain curve for concrete in tension

As can be seen, the tensile stress within the concrete increases to a maximum where cracking occurs. After this point, the stress linearly decreases to zero as the concrete crack widens with increasing strain.

The tension stiffening value is an important parameter. The value of total strain, for this model, was taken to be 0.1, as suggested by Basker et al. (2002) and Liang et al. (2004).

4.5 Shear Retention

The shear retention model ensures that the shear modulus of the concrete reduces due to the effect of cracking. So, as the crack widens, the shear stiffness linearly reduces to zero. The shear modulus of cracked concrete is defined by the function:

$$G = \varphi G_c \quad (4.3)$$

where, G_c is the elastic shear modulus of uncracked concrete and φ is a reduction factor. The reduction factor is defined further by:

$$\varphi = \begin{cases} (1 - \varepsilon_c / \varepsilon_{\max}) & \text{For } \varepsilon < \varepsilon_{\max} \\ 0 & \text{For } \varepsilon \geq \varepsilon_{\max} \end{cases} \quad (4.4)$$

The parameters of ε_{\max} and φ were taken as 0.005 and 0.95, respectively, as suggested by Thevendran (1999) and Liang et al. (2004, 2005).

4.6 Conclusions

The composite beam model developed, using the material properties and theories outlined above, should adequately model the behaviour of steel-concrete composite beams. The material properties and theories, as mentioned above, have been used with success by numerous academics in their subsequent experiments, and as such, they should be adequate for use in the present study. Table 4.1 below, summarises the material properties adopted in the current study.

Table 4.1 Material Property Summary

Material	Property	Value
Structural Steel	Yield Stress, f_{sy} (MPa)	265
	Ultimate Strength, f_{su} (MPa)	410

	Young's Modulus, E_s (MPa)	205,350
	Poisson's ratio, ν	0.3
	Ultimate Strain, ε_{su}	0.2
Reinforcing Bars	Yield Stress, f_{sy} (MPa)	250
	Ultimate Strength, f_{su} (MPa)	350
	Young's Modulus, E_s (MPa)	200,000
	Poisson's ratio, ν	0.3
	Ultimate Strain, ε_{su}	0.2
Shear Connectors	Spacing (mm)	110
	Number of rows	2
	Yield Stress, f_{sy} (MPa)	410
	Ultimate Strength, f_{su} (MPa)	580
	Young's Modulus, E_s (MPa)	200,000
	Poisson's ratio, ν	0.3
	Ultimate Strain, ε_{su}	0.2
Concrete	Compressive strength, f'_c (MPa)	42.5
	Tensile Strength, f_{ct} (MPa)	3.553
	Young's Modulus, E_c (MPa)	35,709
	Poisson's ratio, ν	0.15
	Ultimate compressive strain, ε_{cu}	0.0045

Chapter 5. Results & Discussion

5.1 Introduction

All results were obtained using the finite element analysis method through the use of the program, ABAQUS. The model generated was used to create input files that are used by ABAQUS for analysis. The input files, once generated, were further edited to apply additional controls, as previously mentioned. The results obtained were then transported to a spreadsheet for further minor computations and for result presentation.

5.2 Model Validation

The model validation step is an important procedure. It ensures that the model generated can be relied upon when further analysis is conducted.

The model validation was done by the comparison of existing load/deflection data by Chapman and Balakrishnan (1964). The model was intentionally modelled to the geometry of the beam tested by Chapman and Balakrishnan. The shear connectors' cross-sectional area was altered to make them behave in accordance with the shear connectors used in the experiment.

The model was loaded as a simply supported steel-concrete composite beam with a single point load at mid-span. The point load in the model was modelled as an equivalent pressure over an area of 120 mm x 120 mm. Deflection was monitored at the bottom of the joist at mid-span and the load applied was automatically stepped up until the point of failure.

Table 5.1 summarises the load/deflection data obtained from the model.

Table 5.1 Load/deflection data

Deflection	Load factor	Load
0.994	0.049993	25.91637
1.99	0.099969	51.82393
3.48	0.1749	90.66816
5.47	0.2745	142.3008
7.46	0.3738	193.7779
9.46	0.4728	245.0995
11.5	0.5711	296.0582
13.5	0.6604	342.3514
15.6	0.7116	368.8934
17.8	0.7467	387.0893
19.9	0.7732	400.8269
22.1	0.797	413.1648
24.2	0.8174	423.7402
26.4	0.8344	432.553
28.5	0.8507	441.0029
29.1	0.854	442.7136
29.6	0.8578	444.6835
30.1	0.8615	446.6016
30.9	0.8669	449.401
32.1	0.8748	453.4963
34	0.8865	459.5616
34.6	0.8904	461.5834
34.9	0.8926	462.7238
35.5	0.8959	464.4346

36.3	0.9005	466.8192
37.5	0.9065	469.9296
39.3	0.914	473.8176
40.3	0.9172	475.4765
40.9	0.9176	475.6838
41.8	0.9164	475.0618
43.1	0.9116	472.5734
43.8	0.9081	470.759
44.9	0.9024	467.8042
45.5	0.8996	466.3526
46.4	0.8963	464.6419
47.8	0.8929	462.8794
48.6	0.8917	462.2573
49.7	0.8903	461.5315
51.4	0.8895	461.1168
54	0.8887	460.7021
57.9	0.888	460.3392
60.1	0.8878	460.2355
63.4	0.8875	460.08
65.2	0.8873	459.9763
68	0.8872	459.9245
72.2	0.8872	459.9245
74.5	0.8872	459.9245
78.1	0.8871	459.8726
80.1	0.8871	459.8726

Figure 5.1 graphically compares the results above with those obtained by Chapman and Balakrishnan. Figure 5.2 shows the graphical results obtained from ABAQUS.

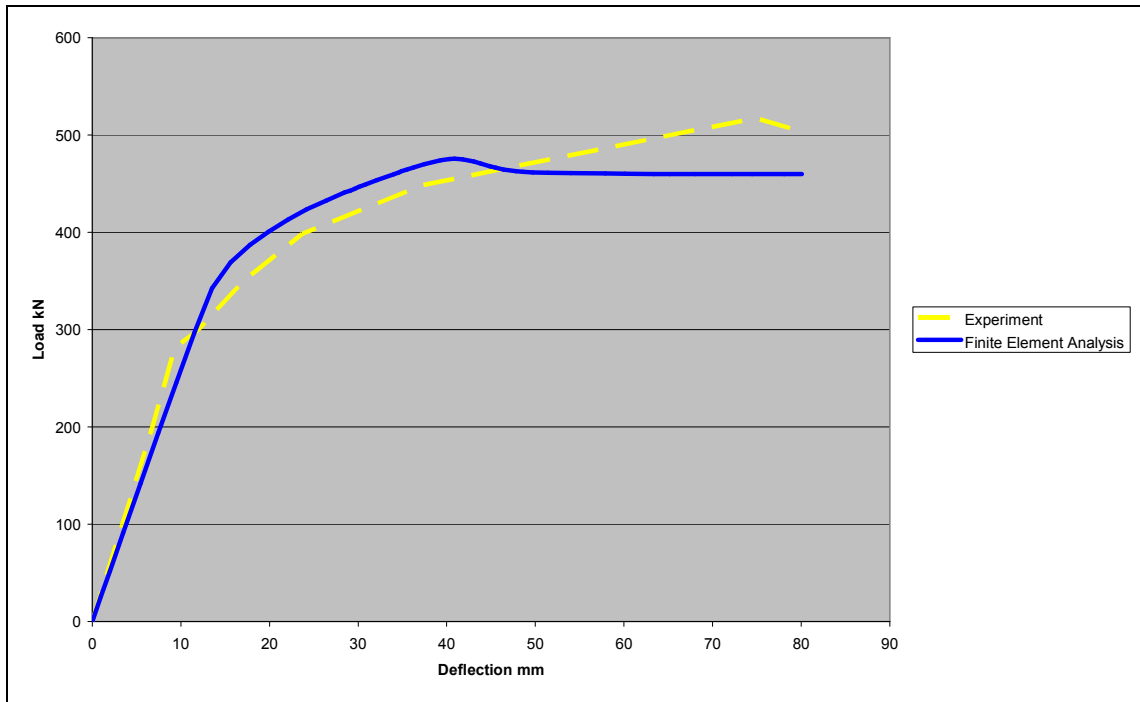


Figure 5.1 Comparison of Load/Deflection Results

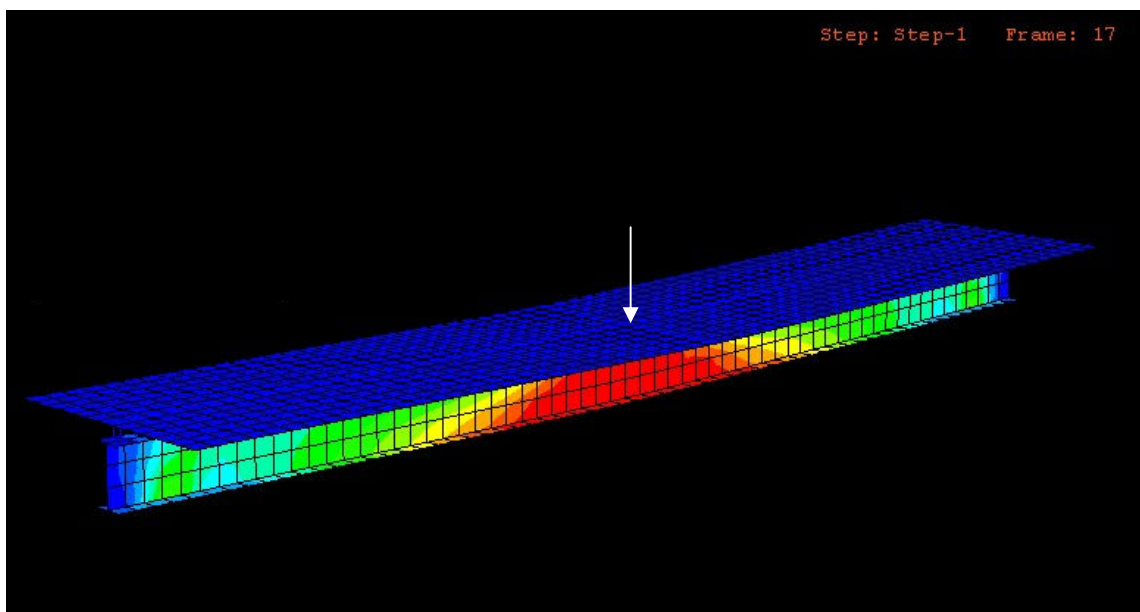


Figure 5.2 Steel-Concrete Composite Beam Under Pure Flexure

The beam tested by Chapman and Balakrishnan obtained an ultimate load of 517.1316 kN and the ultimate load obtained from the finite element model was 475.6838 kN. Comparing those values:

$$Difference(\%) = \left[1 - \left(\frac{475.6838}{517.1316} \right) \right] \times 100 = 8.015\% \quad (5.1)$$

Therefore, the finite element model estimated an ultimate load that is 8.015 % lower than that achieved by Chapman and Balakrishnan. Therefore it can be concluded that the model created is reliable and conservative in predicting the ultimate load.

5.3 Moment-Torque Interaction

A further 15 different loading schemes were tested to explore the behaviour of steel-concrete composite beams under both flexure and torsion. Each load case had the simulated point load's eccentricity increased up to the maximum eccentricity, as defined by the slab geometry. The eccentricity stated in each model, refers to the eccentric length " l " as described in figure 3.1.

5.3.1 Boundary Conditions

For analysing both flexure and torsion, a different boundary condition scheme is required than that used in the case of simple flexure. As mentioned in the literature, the contribution to total torsional strength added by the steel joist is negligible when compared to the torsional strength supplied by the concrete slab. As a result of this, any torsional forces induced in the beam needs to be transferred to boundary conditions not directly associated with the steel joist, otherwise all torsional forces generated needs to reach the boundary conditions through the steel joist, neglecting the torsional strength the concrete supplies. Figure 5.3 graphically represents the boundary conditions used in the simple flexure case.

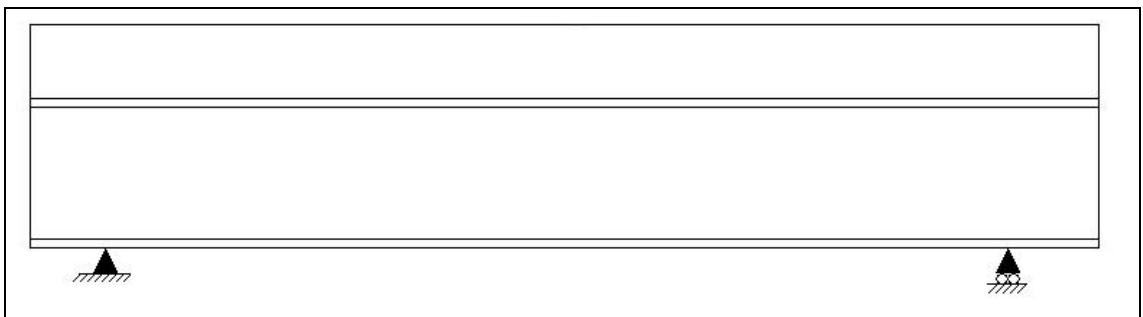


Figure 5.3 Simply Supported Composite Beam

If the above support conditions were employed, the concrete slab would offer no resistance to torsion. Any torsion imposed on the beam above would be solely resisted by the steel joist. As the torsion increases, the concrete slab would

just rotate with the upper flange, as the lower flange-web connection operates as a pivot point. Figure 5.4 graphically represents the boundary conditions adopted in the current study.

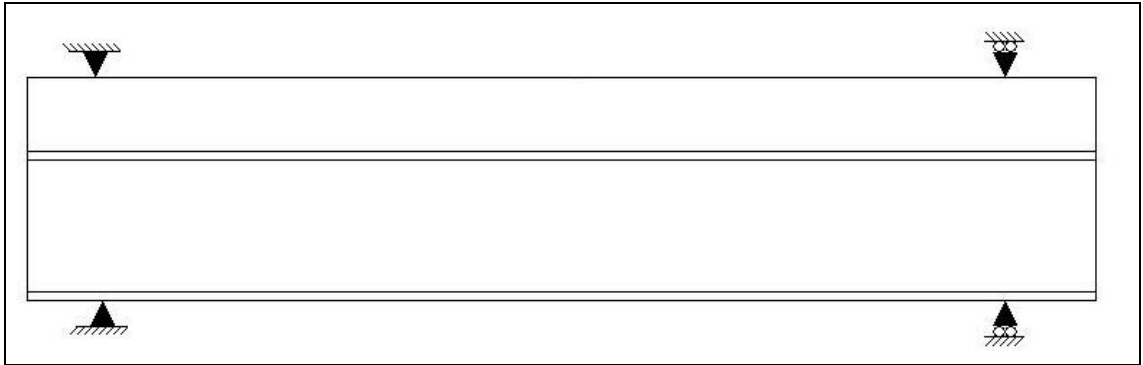


Figure 5.4 Adopted Boundary Conditions for the Composite Beam

The adopted support conditions, displayed above, allow the concrete slab to resist torsional forces. Subsequently, the above support conditions also increases the beams capacity to resist pure flexure, therefore any results obtained in the model validation phase, are not able to be included within the analysis of flexure and torsion.

5.3.2 Load-Deflection Curves

Load-deflection curves were generated for each load scheme. ABAQUS monitored and recorded the load scale factors and the deflections at mid-span. The subsequent results were then graphed. Figures 5.5 to 5.9, display the load-deflection results for the fifteen loading schemes.

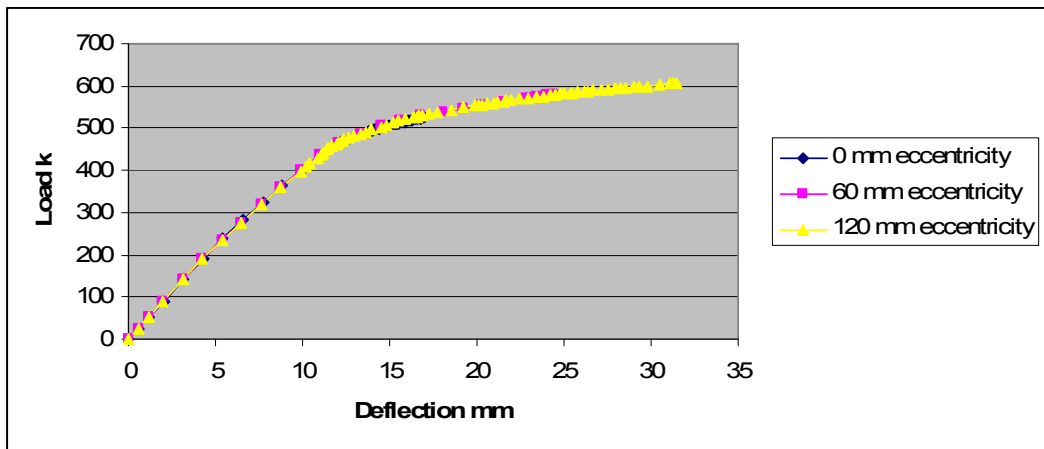


Figure 5.5 Load/Deflection Curve 1

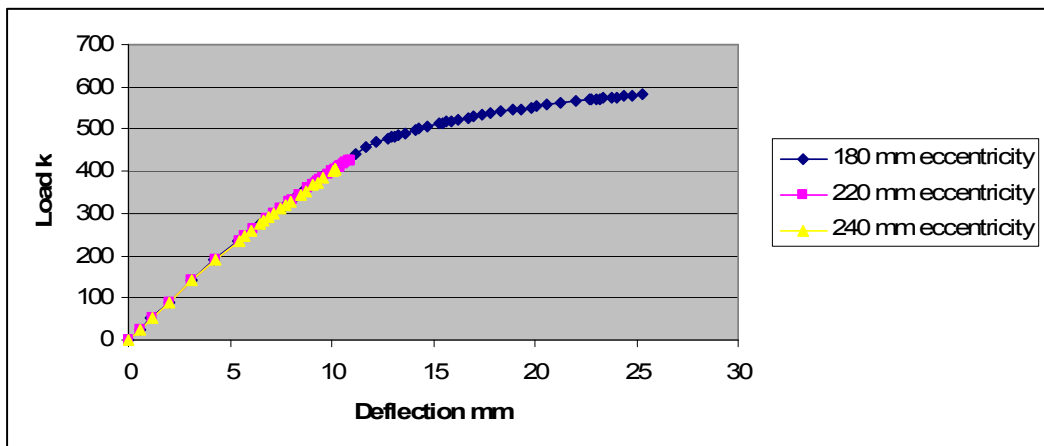


Figure 5.6 Load/Deflection Curve 2

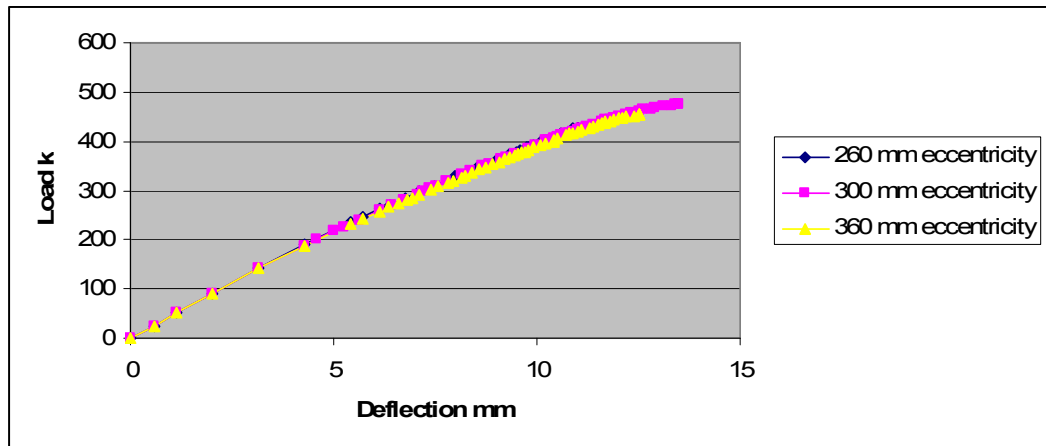


Figure 5.7 Load/Deflection Curve 3

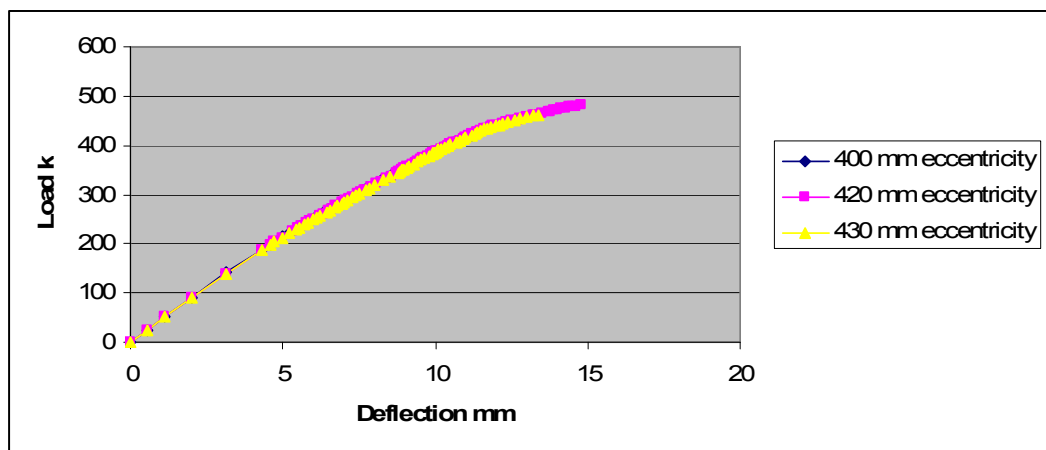


Figure 5.8 Load Deflection Curve 4

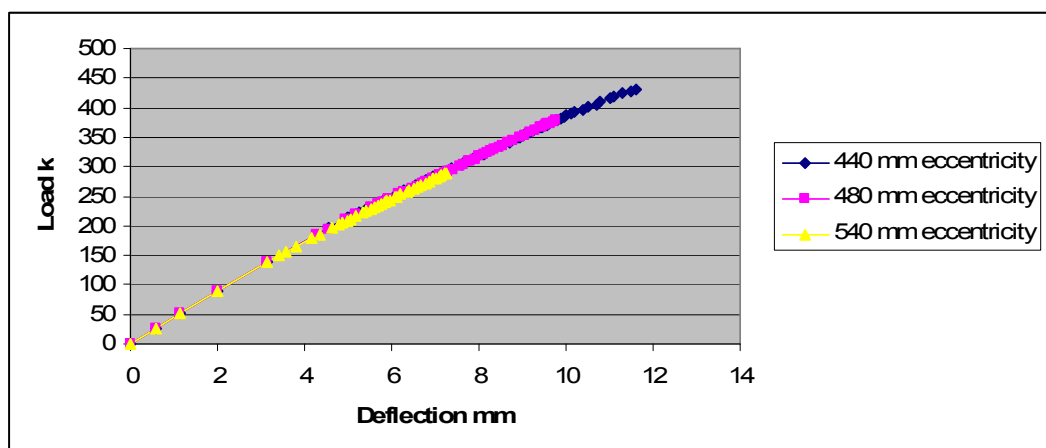


Figure 5.9 Load/Deflection Curve 5

From the above curves, it can be noted that as the eccentricity increases, the deflection increases at a greater rate. This is because as the eccentricity increases, the imposed torque greatly increases and because the loading scheme becomes further removed from the optimum loading arrangement. It can also be seen that the load schemes have a non-consistent termination point, the point where the analysis ended. This anomaly will be discussed later. Appendix 1 contains the Load/Deflection tables for the loading schemes plotted in figures 5.5 to 5.9 above.

5.3.3 Moment-Torque Curves

From the Load/Deflection data, contained in Appendix 1, values of moment and torque were calculated using formulas 3.1 and 3.2. The results for each load case was then plotted to define a relationship between moment and torque. Initially, ten load cases were analysed, each time with the eccentricity increasing by 60 mm. Figure 5.6 describes the initial moment/torque diagram obtained from the first ten results.

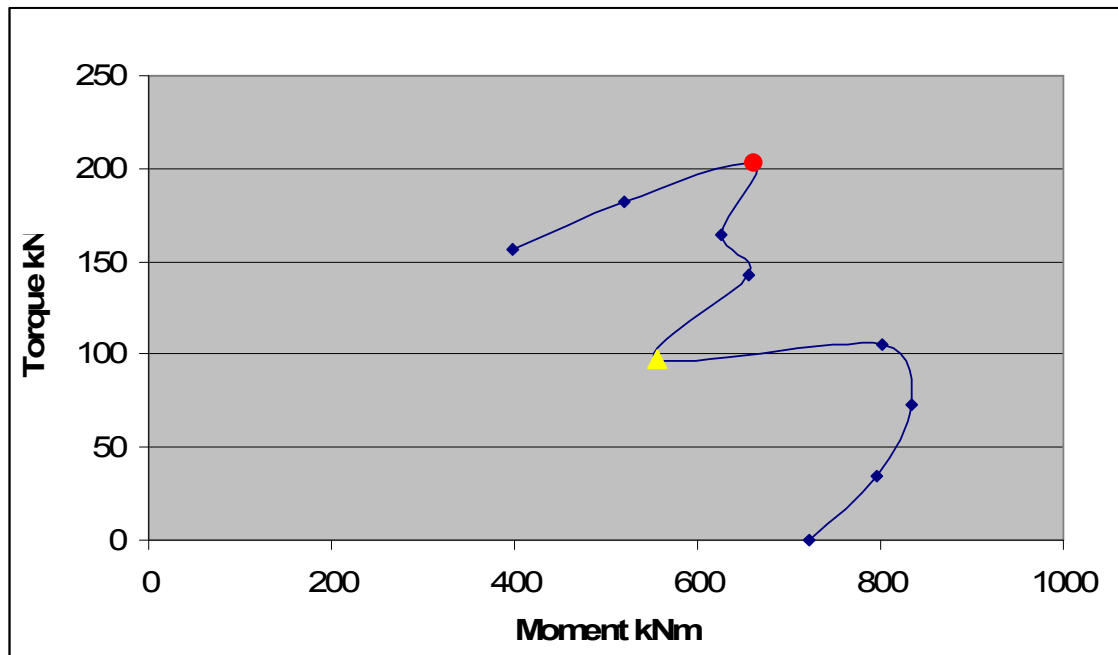


Figure 5.10 Initial Moment/Torque Diagram

Starting from the point of zero torque, the conceding points represent the ultimate moment and torque achieved with increasing eccentricity. Again, these points represent an eccentricity that is increasing by 60 mm.

This initial diagram, in figure 5.10, looked as though to be making a nice curve, neglecting the point marked yellow as a triangle (eccentricity of 240 mm), and the point marked red as a circle (eccentricity of 420 mm). It was thought that those two points, being so far removed from the general pattern, may be incorrect and it was decided to check the two input files that generated that data and run further analysis at eccentricities similar to those points. This led to the analyses of load cases with eccentricities of 220, 260, 400, 430 and 440 mm eccentricities. At the conclusion of these analyses, their data was also plotted, creating the curve as seen in figure 5.11.

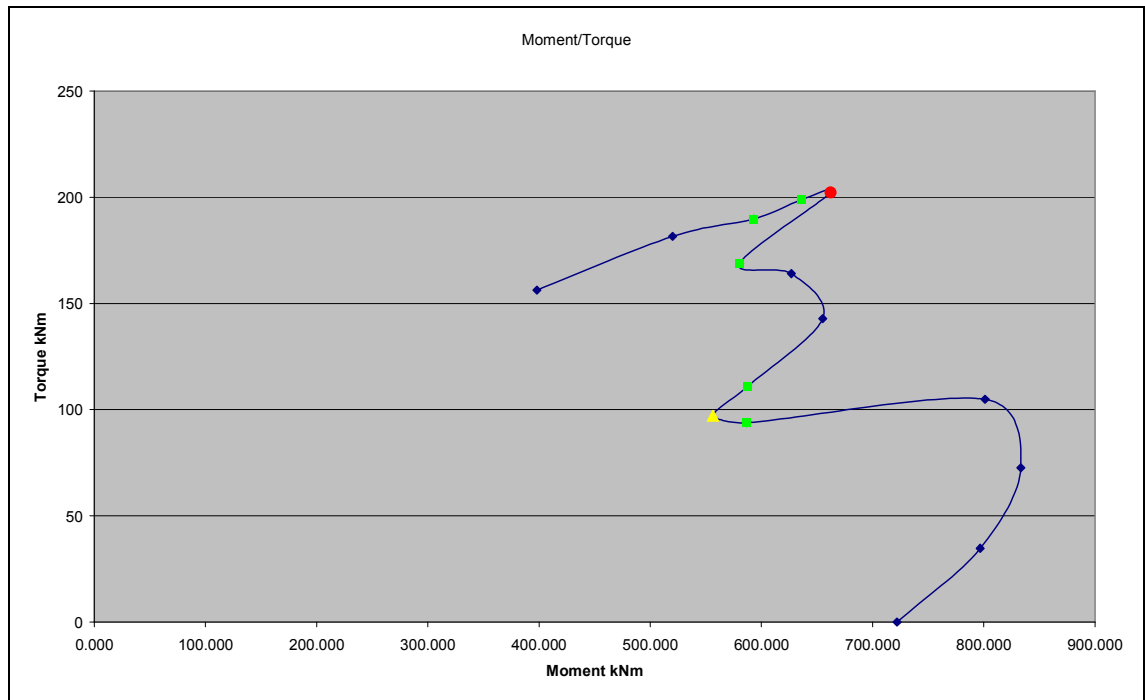


Figure 5.11 Moment/Torque Diagram

The new points, plotted in green as squares, work to confirm those initial outlying results. The input files that generated the red circle and the yellow square were also re-tested with new input files, both of which confirmed the results obtained in the initial analysis. From this figure it can be gathered that the model itself is not reliable in testing beams under both bending and torsion.

5.3.4 Model Behaviour

From the ultimate load behaviour, displayed in figure 5.11 above, it can be concluded that the predictions of ultimate load made by the model are inaccurate. The model does however behave in a way that would suggest that it is acting true. The problem seems to lie in the estimation of ultimate behaviour. Figure 5.12

below, shows the composite beam under an eccentric load at a distance of 120 mm.

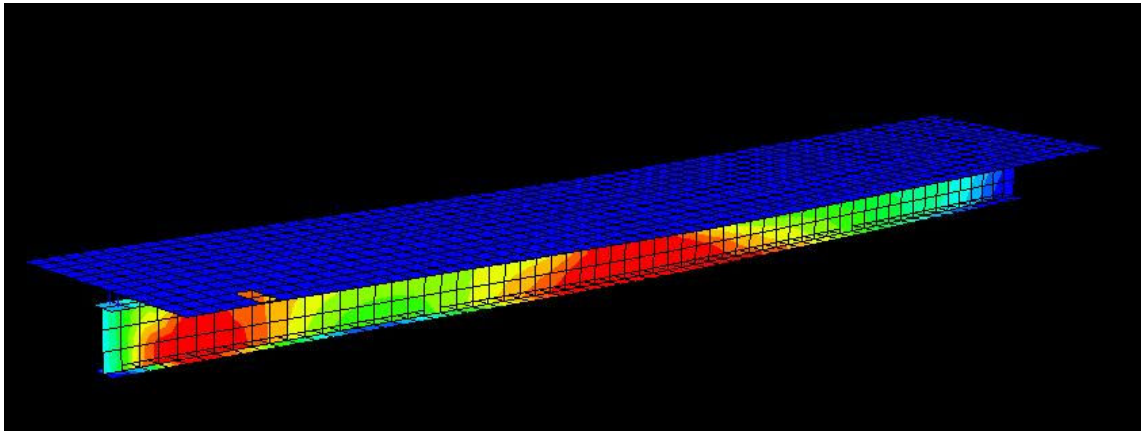


Figure 5.12 Steel-Concrete Composite Beam under 120 mm eccentric load

The arrow indicates the approximate location of the force. It can be seen that an area of high tensional stress exists at the bottom of the joist at mid-span and at the boundary condition location where movement is restricted in every dimension. Figure 5.13 represents the same beam but with the eccentricity increased to 360 mm.

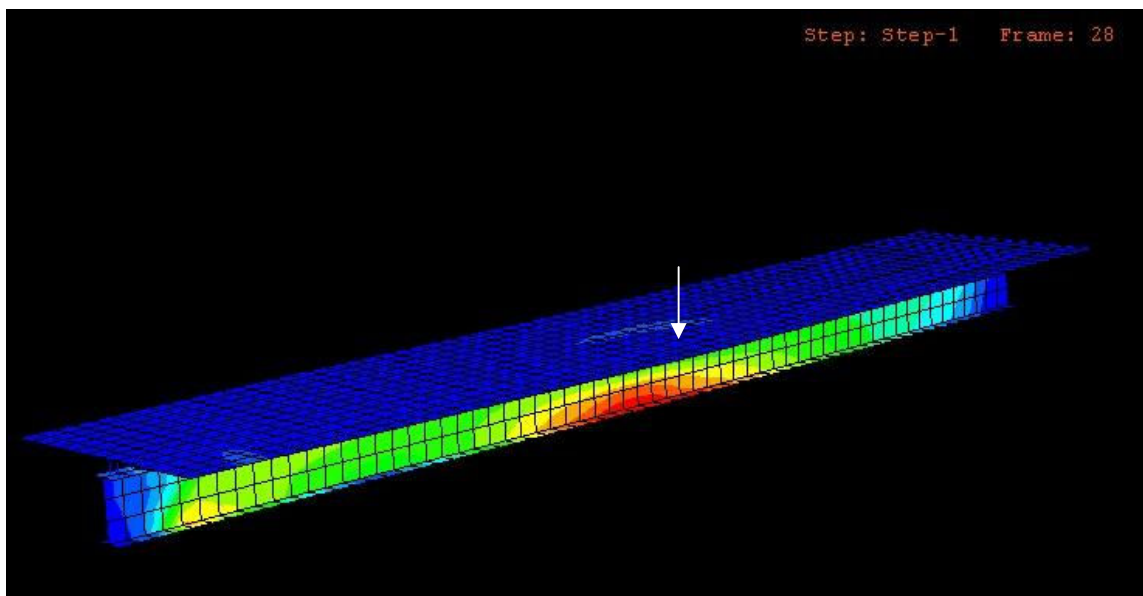


Figure 5.13 Steel-Concrete Composite Beam under 360 mm eccentric load

The arrow displays the approximate location of the eccentric load. From this image, it can be noted that the tensional stress pattern is similar to that represented in figure 5.12, but with lower values of stress. This figure also represents an area of tensional stress developing in the top layer of the concrete slab, perpendicular to the joist location. Figure 5.14 represents the beam under an eccentric load of 400 mm. It has a better representation of the tensional stress area in the concrete slab.

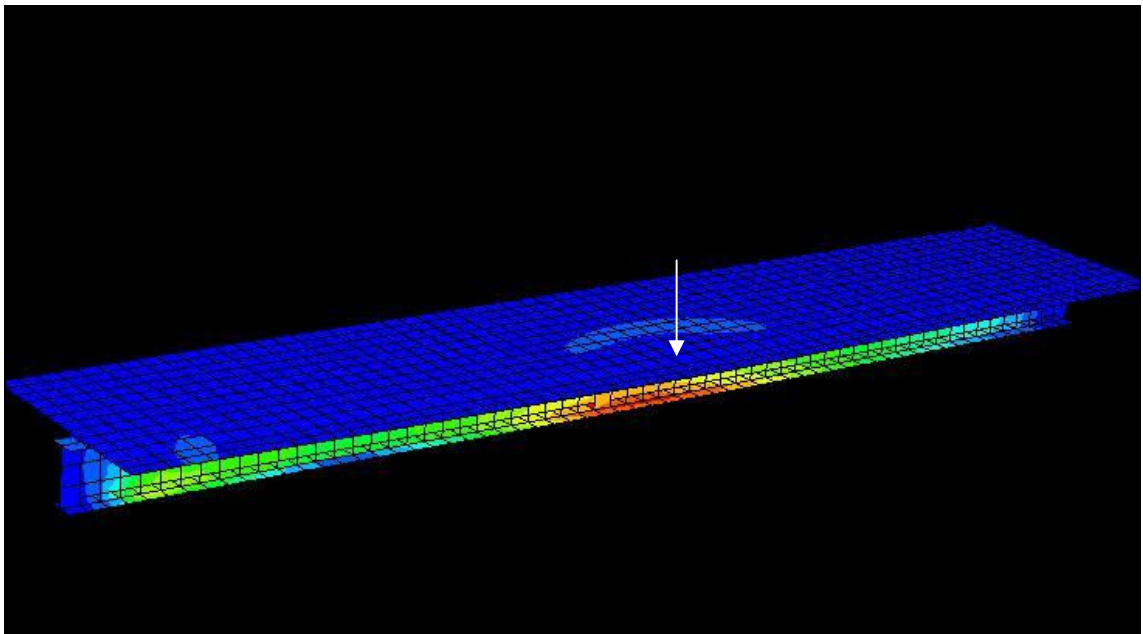


Figure 5.14 Steel-Concrete Composite Beam under 400 mm eccentric load

As can be seen from this figure, a “c” shaped area of tensional stress is developing in the concrete slab. This is because, as the load eccentricity is increased, the concrete slab increasingly acts as a cantilever to resist the load. The development of tensional stress within this region speaks of that. Figure 5.15 describes the cantilever geometry.

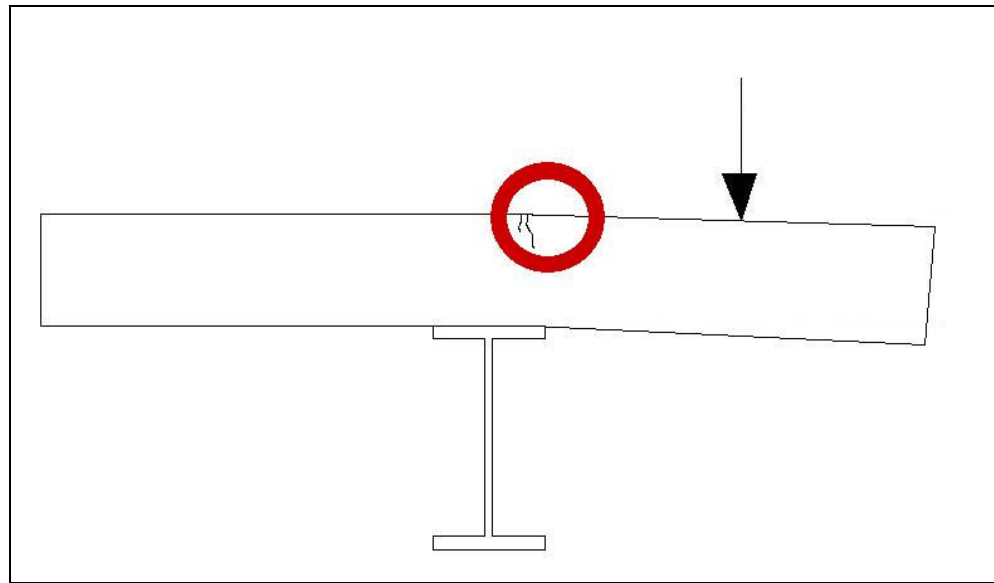


Figure 5.15 Cantilever Arrangement

The circle in red typically describes the area of crack formation in a cantilever orientation. This area is what is being represented as a tensional zone in the concrete slab in figure 5.14. Since the concrete slab and its reinforcement is not designed for a cantilever orientation, the slab has a low ability to resist tension within this area, therefore, greater eccentricities experience failure in this region earlier due to the cantilever effect increasing, i.e. the moment around that axis increasing. So from this behaviour, it can be assumed that the beam is behaving in an appropriate manner and that the problem exists in the estimation of ultimate load.

5.4 Model Inadequacies

The model generated makes use of several material property models, interaction models and geometric configurations in an effort to make a robust, reliable model. Some of these models are simplifications or estimates to the effects seen in practice. These simplifications may have an active part in the ultimate behaviour of the model, as displayed earlier.

5.4.1 Rebar Layers

As mentioned earlier, the steel reinforcing within the concrete slab was modelled using the rebar layers option. This in effect, creates a smeared layer of equivalent area to the reinforcing provided, with the material properties to match. In a simple pure bending arrangement, this is an effective and simple method for modelling reinforcing bars because the moment applied is acting primarily in one direction. In the load case used within this study, bending moment is being applied in around two different axes so in this scenario, a steel reinforcing bar is going to act quite differently to an equivalent area rectangular prism of reinforcing spread across the concrete cross-section at the appropriate depth. So, in a scenario involving axial torsion, the location “x” is just as important as the depth location “y” in a concrete cross-section. In the cantilever arrangement, as described in figure 5.15, longitudinal reinforcement will do little to resist the axial moment created, whereas a rectangular prism of reinforcement will provide much more resistance to that axial moment.

5.4.2 Material Properties and Modelling Techniques

Additional errors could arise out of the material property models and the modelling techniques used. For example, the concrete model may be inadequate for use within this application of bending and torsion or perhaps it is the concrete tension model that is inadequate for use in this application. The model generated may estimate inaccurate ultimate loads as a result of this problem or a combination of them.

5.5 Conclusions

As a result of the uncharacteristic moment-torque curve generated, no design formulas have been prepared to mimic the behaviour of that curve. It can be concluded that though the model is adequate for use in pure flexure load cases, its reliability in moment-torque load cases is not adequate for use. It has been identified that the model has inherent inadequacies which limit the reliability of the results obtained from any moment-torque load case, primarily from the use of rebar layers, a simplification of reinforcement modelling. It has also been identified that the material property models, namely the concrete model, may be inadequate for use under this loading scheme.

Chapter 6. Conclusions

6.1 Summary

This project aimed to study the relationship between moment and torque in steel-concrete composite beams. This relationship was to be studied using the finite element method of analysis, which requires the generation of a model to predict the behaviour of steel-concrete composite beams. The general purpose finite element program ABAQUS was used to conduct the non-linear finite element analysis. Using ABAQUS, a model was created, as described in this paper, to predict steel-concrete composite beam loading behaviour. The created model was compared with existing results for a pure bending case to vilify the reliability of the generated model. From this step, it was found that the model generated was able to accurately predict the ultimate load to within 10% of that achieved in the published experiment. It was hence concluded that the model was reliable and accurate to use.

The model created was then altered to the new loading conditions that induce both flexure and torsion within the beam. This involved changing the boundary conditions to something more appropriate to the loading scheme adopted. In total, fifteen different loading schemes were analysed and graphed.

The graphed results indicating the relationship between moment and torque were considered incorrect and therefore inappropriate for the development of design formulas. It was identified that the use of rebar layers, for modelling the reinforcement, was inappropriate for use in the case of flexure and torsion, and it

was considered that perhaps the concrete model was inappropriate for use in the analysed loading scheme of flexure and torsion.

6.2 Further Research

Several areas of further research exist, both experimentally and computationally. Further research should be conducted in testing steel-concrete composite beams under flexure and torsion in a similar loading scheme to that used within this study. That is similar to that shown in figure 6.1, as opposed to that shown in figure 6.2. Where “F” is the applied force and “M” is the torque.

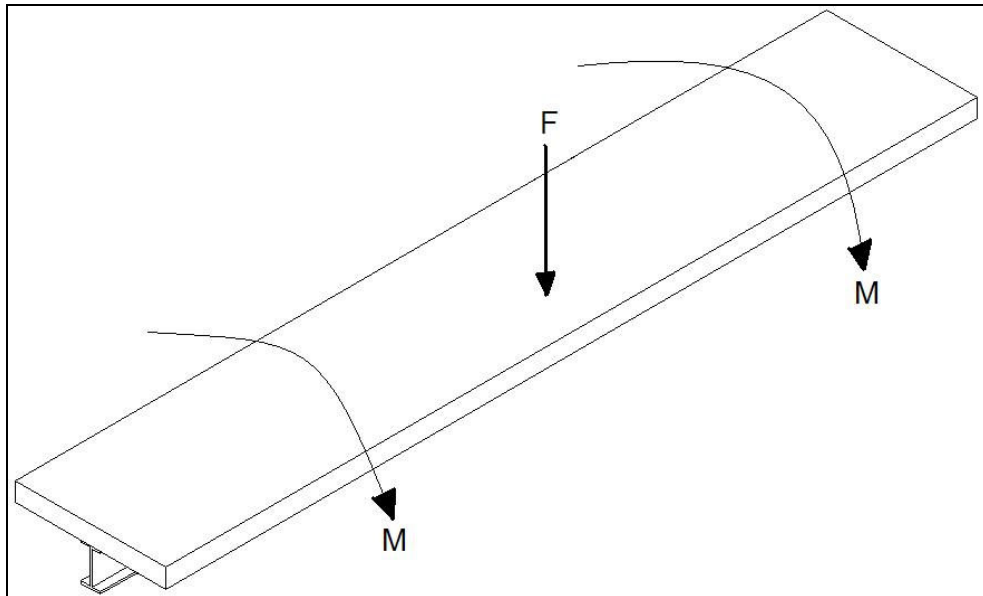


Figure 6.1 Suggested Loading Scheme

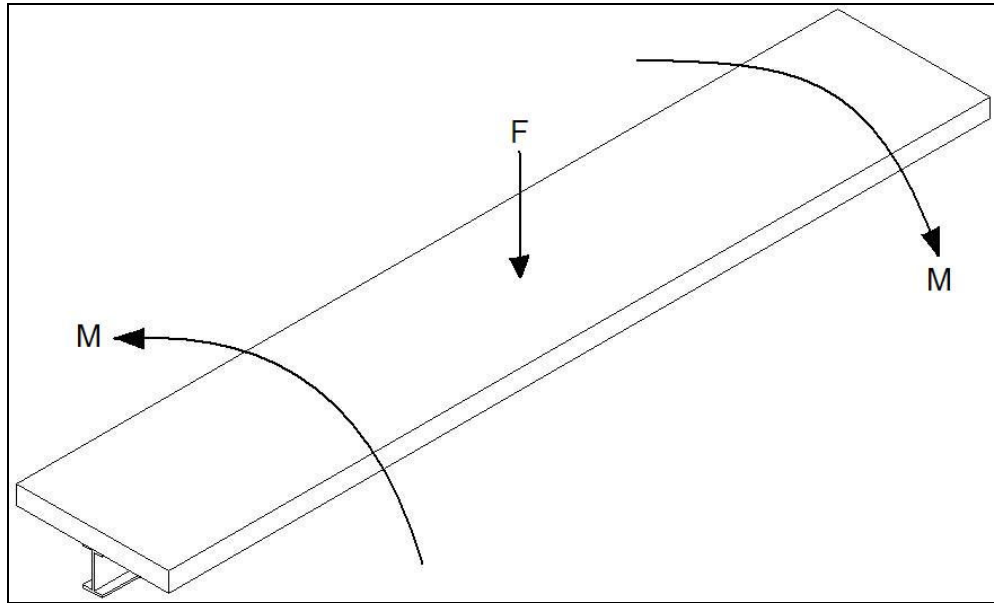


Figure 6.2 Alternative Loading Scheme

From this experimental study, appropriate load/deflection graphs and moment/torque interaction graphs should be generated to provide information for subsequent computational analysis and for the generation of appropriate design formulas for designing steel-concrete composite beams under both flexure and torsion.

Appendices

Appendix A, Project Specification

University of Southern Queensland

FACULTY OF ENGINEERING AND SURVEYING

ENG 4111/4112 Research Project
PROJECT SPECIFICATION

FOR: Matthew KRONK

TOPIC: ULTIMATE STRENGTH OF STEEL-CONCRETE
COMPOSITE BEAMS UNDER COMBINED BENDING
AND TORSION (Project No. 06-217)

SUPERVISOR: Dr. Qing Quan (Stephen) Liang

PROJECT AIM: This project aims to investigate the ultimate load behaviour of steel-concrete composite beams under the combined actions of bending and torsion using the finite element analysis programs. The results obtained will then be used to develop design formulas for the design of composite beams under bending and torsion.

PROGRAMME: **Issue A, 21st March 2006**

1. Conduct a literature review on the experimental behaviour of composite beams and on the nonlinear finite element analysis of composite beams.
2. Research into any experiments conducted on composite beams, particularly on similar loading conditions to obtain data for verification.
3. Study the nonlinear finite element analysis method and develop a three-dimensional finite element model for the nonlinear analysis of composite beams under combined bending and torsion.
4. Conduct nonlinear finite element analyses on composite beams with full shear connections under combined bending and torsion.
5. Generate the ultimate moment-torque interaction diagram to display the interaction strengths of composite beams under combined actions.
6. Develop design formulas from the results that can be used for designing composite beams under similar loading conditions.

Time permitting:

7. Modify the finite element models for composite beams with partial shear connections and conduct nonlinear analyses.

AGREED: _____ (Student) _____ (Supervisor)

Appendix B, Load/Deflection Tables

0 mm eccentricity			60 mm eccentricity		
Deflection	load factor	load	Deflection	load factor	load
0	0	0	0	0	0
0.573	5.00E-02	25.9194816	0.566	5.00E-02	25.9314048
1.15	0.1	51.84	1.13	0.1001	51.89184
2.01	0.175	90.72	1.98	0.1752	90.82368
3.15	0.2741	142.09344	3.12	0.2739	141.98976
4.3	0.3691	191.34144	4.25	0.3653	189.37152
5.44	0.4582	237.53088	5.37	0.4516	234.10944
6.58	0.5433	281.64672	6.5	0.5342	276.92928
7.72	0.624	323.4816	7.62	0.6145	318.5568
8.86	0.7019	363.86496	8.75	0.6935	359.5104
9.99	0.7755	402.0192	9.87	0.7697	399.01248
11.1	0.8445	437.7888	11	0.8418	436.38912
12.3	0.9016	467.38944	12.1	0.9008	466.97472
12.6	0.9118	472.67712	13.3	0.9396	487.08864
13	0.9254	479.72736	14.5	0.9723	504.04032
13.7	0.9439	489.31776	15.6	0.9997	518.24448
13.7	0.9449	489.83616	16.8	1.021	529.2864
13.8	0.9463	490.56192	18	1.04	539.136
13.8	0.9485	491.7024	19.2	1.057	547.9488
14	0.9517	493.36128	20.3	1.073	556.2432
14.1	0.9565	495.8496	21.5	1.088	564.0192
14.2	0.9592	497.24928	22.7	1.101	570.7584
14.4	0.9631	499.27104	23	1.104	572.3136
14.6	0.9687	502.17408	23.4	1.108	574.3872
14.7	0.9718	503.78112	23.7	1.111	575.9424
14.9	0.976	505.9584	24	1.114	577.4976
15	0.9781	507.04704	24.1	1.115	578.016
15.2	0.9813	508.70592	24.2	1.116	578.5344
15.3	0.983	509.5872	24.4	1.117	579.0528
15.4	0.9857	510.98688	24.4	1.117	579.0528
15.5	0.9871	511.71264	24.4	1.117	579.0528
15.6	0.9892	512.80128	24.4	1.117	579.0528
15.8	0.9923	514.40832	24.4	1.117	579.0528
15.9	0.9939	515.23776	24.4	1.118	579.5712
16	0.9964	516.53376	24.4	1.117	579.0528
16.1	0.9978	517.25952	24.4	1.117	579.0528
16.2	0.9999	518.34816	24.4	1.117	579.0528
16.3	1.001	518.9184	24.4	1.117	579.0528
16.4	1.003	519.9552	24.4	1.117	579.0528
16.5	1.005	520.992			
16.6	1.006	521.5104			
16.8	1.008	522.5472			
16.8	1.01	523.584			
16.9	1.011	524.1024			
17	1.012	524.6208			
17	1.013	525.1392			

17	1.013	525.1392			
120 mm eccentricity			180 mm eccentricity		
Deflection	load factor	load	Deflection	load factor	load
0	0	0	0	0	0
0.566	5.00E-02	25.9314048	0.565	5.00E-02	25.9314048
1.13	0.1001	51.89184	1.13	0.1001	51.89184
1.98	0.1752	90.82368	1.98	0.1751	90.77184
3.12	0.2736	141.83424	3.11	0.2731	141.57504
4.25	0.3646	189.00864	4.24	0.3635	188.4384
5.38	0.4509	233.74656	5.37	0.4496	233.07264
6.5	0.5336	276.61824	6.5	0.532	275.7888
7.63	0.6138	318.19392	7.62	0.6118	317.15712
8.75	0.6924	358.94016	7.91	0.6315	327.3696
9.88	0.7682	398.23488	8.19	0.651	337.4784
10.2	0.7866	407.77344	8.61	0.68	352.512
10.4	0.8044	417.00096	9.23	0.7231	374.85504
10.9	0.8307	430.63488	9.59	0.7469	387.19296
11.1	0.8454	438.25536	10.1	0.7815	405.1296
11.2	0.8536	442.50624	10.6	0.8152	422.59968
11.4	0.8653	448.57152	11.2	0.848	439.6032
11.5	0.8716	451.83744	11.7	0.8781	455.20704
11.7	0.8804	456.39936	12.2	0.9033	468.27072
12	0.8925	462.672	12.8	0.9227	478.32768
12.1	0.8988	465.93792	12.9	0.9268	480.45312
12.3	0.9079	470.65536	13.1	0.9309	482.57856
12.4	0.9125	473.04	13.3	0.9368	485.63712
12.6	0.9188	476.30592	13.6	0.9456	490.19904
12.9	0.9277	480.91968	14.1	0.9585	496.8864
13.3	0.94	487.296	14.3	0.9655	500.5152
13.6	0.9468	490.82112	14.7	0.9758	505.85472
13.9	0.9568	496.00512	15.3	0.9904	513.42336
14.5	0.9712	503.47008	15.5	0.994	515.2896
14.8	0.9789	507.46176	15.6	0.9972	516.94848
15.2	0.9901	513.26784	15.9	1.002	519.4368
15.5	0.9956	516.11904	16.2	1.008	522.5472
15.9	1.003	519.9552	16.7	1.017	527.2128
16.4	1.014	525.6576	17	1.022	529.8048
16.6	1.017	527.2128	17.4	1.029	533.4336
16.7	1.019	528.2496	17.8	1.036	537.0624
16.9	1.023	530.3232	18.3	1.043	540.6912
17.3	1.028	532.9152	18.9	1.052	545.3568
17.7	1.036	537.0624	19.3	1.057	547.9488
18.5	1.047	542.7648	19.8	1.065	552.096
19.2	1.058	548.4672	20.1	1.069	554.1696
19.9	1.068	553.6512	20.6	1.075	557.28
20.1	1.07	554.688	21.3	1.083	561.4272
20.3	1.072	555.7248	22	1.091	565.5744
20.6	1.076	557.7984	22.7	1.099	569.7216
21	1.081	560.3904	22.8	1.1	570.24

21.2	1.084	561.9456	23	1.102	571.2768
21.6	1.088	564.0192	23.2	1.104	572.3136
21.7	1.09	565.056	23.4	1.107	573.8688
22	1.093	566.6112	23.8	1.11	575.424
22.5	1.098	569.2032	24	1.112	576.4608
22.9	1.103	571.7952	24.4	1.115	578.016
23.4	1.107	573.8688	24.8	1.12	580.608
23.8	1.111	575.9424	25.3	1.124	582.6816
24.2	1.115	578.016			
24.5	1.118	579.5712			
24.8	1.121	581.1264			
25	1.123	582.1632			
25.4	1.126	583.7184			
25.5	1.127	584.2368			
25.8	1.129	585.2736			
26.2	1.132	586.8288			
26.4	1.134	587.8656			
26.7	1.136	588.9024			
27.2	1.14	590.976			
27.5	1.142	592.0128			
27.9	1.145	593.568			
28.2	1.147	594.6048			
28.5	1.15	596.16			
29	1.153	597.7152			
29.3	1.155	598.752			
29.8	1.158	600.3072			
30.5	1.163	602.8992			
31.1	1.167	604.9728			
31.3	1.168	605.4912			
31.5	1.169	606.0096			
220 mm eccentricity			240 mm eccentricity		
Deflection	load factor	load	Deflection	load factor	load
0	0	0	0	0	0
0.573	5.00E-02	25.9194816	0.572	5.00E-02	25.9194816
1.15	0.1	51.84	1.14	1.00E-01	51.837408
2	0.1749	90.66816	2	0.1748	90.61632
3.15	0.2733	141.67872	3.15	0.2731	141.57504
4.3	0.3664	189.94176	4.3	0.3658	189.63072
5.45	0.4544	235.56096	5.44	0.4535	235.0944
5.73	0.476	246.7584	5.73	0.475	246.24
6.16	0.5079	263.29536	6.01	0.4961	257.17824
6.8	0.5539	287.14176	6.44	0.5271	273.24864
7.16	0.5792	300.25728	6.68	0.5441	282.06144
7.52	0.6041	313.16544	6.92	0.5609	290.77056
7.88	0.6286	325.86624	7.16	0.5775	299.376
8.08	0.6422	332.91648	7.52	0.6021	312.12864
8.38	0.6624	343.38816	7.72	0.6158	319.23072
8.83	0.6923	358.88832	8.01	0.6361	329.75424
9.08	0.709	367.5456	8.46	0.6662	345.35808

9.22	0.7183	372.36672	8.71	0.6828	353.96352
9.3	0.7235	375.0624	9.09	0.7075	366.768
9.42	0.7313	379.10592	9.3	0.7213	373.92192
9.6	0.7428	385.06752	9.62	0.7416	384.44544
9.87	0.76	393.984	10.1	0.7716	399.99744
10	0.7697	399.01248	10.2	0.7791	403.88544
10.2	0.7839	406.37376	10.2	0.7792	403.93728
10.3	0.7875	408.24	10.2	0.7794	404.04096
10.4	0.791	410.0544	10.2	0.7796	404.14464
10.4	0.7962	412.75008	10.2	0.78	404.352
10.6	0.804	416.7936	10.2	0.7806	404.66304
10.7	0.8113	420.57792	10.2	0.7807	404.71488
10.8	0.819	424.5696	10.2	0.7807	404.71488
10.9	0.8209	425.55456	10.2	0.7807	404.71488
10.9	0.8228	426.53952			
10.9	0.8229	426.59136			
10.9	0.8229	426.59136			
260 mm eccentricity			300 mm eccentricity		
Deflection	load factor	load	Deflection	load factor	load
0	0	0	0	0	0
0.572	5.00E-02	25.9194816	0.572	5.00E-02	25.9194816
1.14	1.00E-01	51.8363712	1.14	1.00E-01	51.834816
2	0.1748	90.61632	2	0.1748	90.61632
3.15	0.2729	141.47136	3.15	0.2725	141.264
4.3	0.3652	189.31968	4.3	0.3639	188.64576
5.44	0.4525	234.576	4.58	0.3858	199.99872
5.73	0.4738	245.61792	5.01	0.4183	216.84672
6.15	0.5052	261.89568	5.25	0.4363	226.17792
6.39	0.5223	270.76032	5.61	0.463	240.0192
6.75	0.5476	283.87584	6.14	0.5021	260.28864
7.1	0.5724	296.73216	6.44	0.5233	271.27872
7.46	0.5968	309.38112	6.74	0.544	282.0096
7.99	0.6326	327.93984	7.04	0.5643	292.53312
8.51	0.6677	346.13568	7.2	0.5756	298.39104
9.04	0.702	363.9168	7.37	0.5869	304.24896
9.33	0.7211	373.81824	7.53	0.5981	310.05504
9.49	0.7317	379.31328	7.78	0.6146	318.60864
9.59	0.7376	382.37184	8.15	0.639	331.2576
9.73	0.7465	386.9856	8.36	0.6527	338.35968
9.8	0.7515	389.5776	8.66	0.6729	348.83136
9.92	0.7588	393.36192	8.84	0.6843	354.74112
10.1	0.7699	399.11616	9.1	0.701	363.3984
10.4	0.7863	407.61792	9.24	0.7104	368.27136
10.6	0.8024	415.96416	9.46	0.7243	375.47712
10.9	0.8176	423.84384	9.78	0.7449	386.15616
10.9	0.8214	425.81376	9.96	0.7563	392.06592
11	0.8224	426.33216	10.2	0.773	400.7232
11	0.8238	427.05792	10.3	0.777	402.7968
11	0.8246	427.47264	10.4	0.7812	404.97408

11	0.8246	427.47264			
11	0.8247	427.52448			
11	0.8247	427.52448			
10.4	0.7854	407.15136			
10.5	0.7895	409.2768			
10.6	0.7955	412.3872			
10.7	0.7989	414.14976			
10.7	0.799	414.2016			
10.7	0.8011	415.29024			
10.8	0.8031	416.32704			
10.8	0.806	417.8304			
10.9	0.8103	420.05952			
11	0.8164	423.22176			
11.1	0.8252	427.78368			
11.2	0.8301	430.32384			
11.4	0.8373	434.05632			
11.6	0.8481	439.65504			
11.7	0.8541	442.76544			
11.8	0.8574	444.47616			
11.9	0.8623	447.01632			
12	0.8696	450.80064			
12.2	0.8766	454.42944			
12.3	0.8826	457.53984			
12.5	0.888	460.3392			
12.6	0.8932	463.03488			
12.8	0.8983	465.67872			
12.9	0.903	468.1152			
13.1	0.9077	470.55168			
13.3	0.9117	472.62528			
13.4	0.9163	475.00992			
13.5	0.9175	475.632			
13.5	0.9187	476.25408			
13.5	0.919	476.4096			
360 mm eccentricity			400 mm eccentricity		
Deflection	load factor	load	Deflection	load factor	load
0	0	0	0	0	0
0.572	5.00E-02	25.9194816	0.572	5.00E-02	25.91948
1.14	1.00E-01	51.8306688	1.14	1.00E-01	51.82393
2	0.1747	90.56448	2	0.1746	90.51264
3.15	0.2717	140.84928	3.15	0.271	140.4864
4.29	0.3617	187.50528	4.29	0.3598	186.5203
5.42	0.4462	231.31008	4.57	0.381	197.5104
5.7	0.4666	241.88544	4.99	0.4123	213.7363
6.12	0.496	257.1264	5.22	0.4296	222.7046
6.35	0.512	265.4208	5.36	0.4391	227.6294
6.58	0.5277	273.55968	5.55	0.4531	234.887
6.81	0.5431	281.54304	5.66	0.4608	238.8787
6.93	0.5517	286.00128	5.82	0.4722	244.7885
7.12	0.5645	292.6368	6.07	0.489	253.4976
7.41	0.5835	302.4864	6.2	0.4983	258.3187
7.57	0.5941	307.98144	6.4	0.512	265.4208
7.81	0.6097	316.06848	6.52	0.5197	269.4125

7.94	0.6184	320.57856	6.68	0.531	275.2704
8.14	0.6315	327.3696	6.85	0.5422	281.0765
8.25	0.6387	331.10208	7.02	0.5533	286.8307
8.41	0.6493	336.59712	7.26	0.5695	295.2288
8.58	0.66	342.144	7.4	0.5787	299.9981
8.74	0.6702	347.43168	7.6	0.5921	306.9446
8.9	0.6807	352.87488	7.72	0.5997	310.8845
9.06	0.6912	358.31808	7.89	0.6105	316.4832
9.22	0.7015	363.6576	8.05	0.6215	322.1856
9.31	0.7073	366.66432	8.22	0.6323	327.7843
9.45	0.7158	371.07072	8.47	0.648	335.9232
9.52	0.7207	373.61088	8.53	0.652	337.9968
9.63	0.7279	377.34336	8.59	0.656	340.0704
9.7	0.7318	379.36512	8.68	0.6619	343.129
9.79	0.7377	382.42368	8.77	0.6678	346.1875
9.93	0.7467	387.08928	8.86	0.6737	349.2461
10.1	0.7555	391.6512	8.95	0.6795	352.2528
10.2	0.7642	396.16128	9.04	0.6852	355.2077
10.4	0.7727	400.56768	9.13	0.6909	358.1626
10.4	0.7775	403.056	9.21	0.6964	361.0138
10.5	0.7842	406.52928	9.3	0.702	363.9168
10.7	0.7942	411.71328	9.39	0.7075	366.768
10.8	0.7995	414.4608	9.47	0.713	369.6192
10.9	0.8023	415.91232	9.56	0.7185	372.4704
11	0.8067	418.19328	9.64	0.7238	375.2179
11.1	0.8132	421.56288	9.72	0.7291	377.9654
11.3	0.8229	426.59136	9.8	0.7344	380.713
11.4	0.8324	431.51616	9.89	0.7395	383.3568
11.5	0.8348	432.76032	9.97	0.7447	386.0525
11.5	0.8371	433.95264	10	0.7498	388.6963
11.6	0.8406	435.76704	10.1	0.7548	391.2883
11.7	0.8439	437.47776	10.2	0.7598	393.8803
11.7	0.8473	439.24032	10.3	0.7646	396.3686
11.8	0.8507	441.00288	10.4	0.7695	398.9088
11.9	0.8557	443.59488	10.4	0.7742	401.3453
12	0.8605	446.0832	10.5	0.7788	403.7299
12.1	0.8651	448.46784	10.6	0.7832	406.0109
12.2	0.8692	450.59328	10.7	0.7877	408.3437
12.4	0.873	452.5632	10.8	0.792	410.5728
12.5	0.8768	454.53312	10.9	0.7964	412.8538
12.5	0.8778	455.05152	11	0.8028	416.1715
12.5	0.8788	455.56992	11.1	0.8091	419.4374
12.5	0.8791	455.72544	11.1	0.8107	420.2669
12.5	0.8795	455.9328	11.2	0.8123	421.0963
			11.2	0.8132	421.5629
			11.2	0.8137	421.8221
			11.2	0.814	421.9776
			11.2	0.8144	422.185
420 mm eccentricity			430 mm eccentricity		
Deflection	load	load	Deflection	load	load

	factor			factor	
0	0	0	0	0	0
0.572	5.00E-02	25.91948	0.572	0.049999	25.91948
1.14	1.00E-01	51.82082	1.14	0.09996	51.81926
2	0.1745	90.4608	2	0.1745	90.4608
3.15	0.2707	140.3309	3.15	0.2705	140.2272
4.29	0.359	186.1056	4.29	0.3585	185.8464
4.57	0.3803	197.1475	4.57	0.3797	196.8365
4.73	0.392	203.2128	4.72	0.3914	202.9018
4.97	0.4095	212.2848	4.96	0.4087	211.8701
5.32	0.4349	225.4522	5.19	0.4256	220.631
5.51	0.4487	232.6061	5.42	0.4419	229.081
5.62	0.4563	236.5459	5.55	0.4509	233.7466
5.78	0.4675	242.352	5.74	0.4641	240.5894
5.87	0.4738	245.6179	5.85	0.4714	244.3738
6.01	0.4831	250.439	6.01	0.4823	250.0243
6.21	0.4969	257.593	6.1	0.4884	253.1866
6.32	0.5046	261.5846	6.23	0.4975	257.904
6.49	0.5161	267.5462	6.43	0.511	264.9024
6.59	0.5224	270.8122	6.54	0.5184	268.7386
6.73	0.5319	275.737	6.71	0.5295	274.4928
6.94	0.5458	282.9427	6.8	0.5357	277.7069
7.05	0.5535	286.9344	6.93	0.5448	282.4243
7.17	0.561	290.8224	7.01	0.5497	284.9645
7.28	0.5687	294.8141	7.13	0.5572	288.8525
7.46	0.58	300.672	7.3	0.5684	294.6586
7.55	0.5862	303.8861	7.39	0.5747	297.9245
7.65	0.5924	307.1002	7.53	0.5839	302.6938
7.74	0.5986	310.3142	7.74	0.5975	309.744
7.88	0.6078	315.0835	7.86	0.6051	313.6838
8.09	0.6214	322.1338	8.03	0.6165	319.5936
8.21	0.629	326.0736	8.28	0.6333	328.3027
8.38	0.6404	331.9834	8.53	0.6493	336.5971
8.55	0.6513	337.6339	8.77	0.6651	344.7878
8.72	0.6621	343.2326	8.83	0.669	346.8096
8.76	0.6649	344.6842	8.89	0.6728	348.7795
8.8	0.6675	346.032	8.98	0.6785	351.7344
8.86	0.6716	348.1574	9.06	0.6841	354.6374
8.92	0.6755	350.1792	9.15	0.6898	357.5923
8.98	0.6795	352.2528	9.28	0.698	361.8432
9.04	0.6834	354.2746	9.4	0.7062	366.0941
9.1	0.6874	356.3482	9.53	0.7142	370.2413
9.16	0.6912	358.3181	9.65	0.7222	374.3885
9.25	0.6969	361.273	9.78	0.7301	378.4838
9.34	0.7027	364.2797	9.9	0.7379	382.5274
9.43	0.7084	367.2346	9.93	0.7399	383.5642
9.51	0.714	370.1376	9.96	0.7418	384.5491
9.6	0.7195	372.9888	10	0.7447	386.0525
9.69	0.7249	375.7882	10.1	0.749	388.2816
9.77	0.7304	378.6394	10.1	0.753	390.3552

9.86	0.7358	381.4387		10.2	0.7572	392.5325	
9.94	0.7411	384.1862		10.3	0.7612	394.6061	
10	0.7465	386.9856		10.4	0.767	397.6128	
10.1	0.7516	389.6294		10.5	0.7755	402.0192	
10.2	0.7568	392.3251		10.7	0.7839	406.3738	
10.3	0.7618	394.9171		10.7	0.7861	407.5142	
10.4	0.7667	397.4573		10.8	0.7883	408.6547	
10.4	0.7714	399.8938		10.8	0.7914	410.2618	
10.5	0.776	402.2784		10.9	0.7959	412.5946	
10.5	0.7772	402.9005		11	0.8028	416.1715	
10.6	0.779	403.8336		11.2	0.8095	419.6448	
10.6	0.7816	405.1814		11.3	0.8163	423.1699	
10.7	0.7854	407.1514		11.4	0.823	426.6432	
10.8	0.7911	410.1062		11.5	0.8294	429.961	
10.9	0.7967	413.0093		11.6	0.8331	431.879	
11	0.8023	415.9123		11.7	0.838	434.4192	
11.1	0.8079	418.8154		11.8	0.843	437.0112	
11.2	0.8134	421.6666		12	0.8477	439.4477	
11.3	0.8166	423.3254		12.1	0.8521	441.7286	
11.4	0.8211	425.6582		12.2	0.8565	444.0096	
11.4	0.8238	427.0579		12.4	0.8628	447.2755	
11.5	0.8276	429.0278		12.6	0.869	450.4896	
11.6	0.8331	431.879		12.8	0.8749	453.5482	
11.7	0.8386	434.7302		13	0.8808	456.6067	
11.8	0.8438	437.4259		13.2	0.8866	459.6134	
11.9	0.8468	438.9811		13.4	0.8922	462.5165	
12	0.8509	441.1066					
12.2	0.8565	444.0096					
12.3	0.8621	446.9126					
12.5	0.8675	449.712					
12.7	0.8727	452.4077					
12.8	0.8779	455.1034					
13	0.8829	457.6954					
13.2	0.8879	460.2874					
13.3	0.8928	462.8275					
13.5	0.8976	465.3158					
13.7	0.9024	467.8042					
13.8	0.9051	469.2038					
13.9	0.9091	471.2774					
14	0.9113	472.4179					
14.1	0.9145	474.0768					
14.3	0.9175	475.632					
14.4	0.9203	477.0835					
14.5	0.9229	478.4314					
14.6	0.9256	479.831					
14.8	0.9283	481.2307					
14.8	0.929	481.5936					
440 mm eccentricity				480 mm eccentricity			
Deflection	load factor	load		Deflection	load factor	load	

0	0	0	0	0	0
0.572	0.049999	25.91948	0.572	5.00E-02	25.91896
1.14	0.099958	51.81823	1.14	9.99E-02	51.81304
2	0.1745	90.4608	2	0.1744	90.40896
3.15	0.2703	140.1235	3.15	0.2693	139.6051
4.28	0.3579	185.5354	4.27	0.3554	184.2394
4.56	0.3791	196.5254	4.55	0.3761	194.9702
4.98	0.4098	212.4403	4.95	0.4055	210.2112
5	0.4114	213.2698	5.18	0.4212	218.3501
5.04	0.4138	214.5139	5.51	0.4439	230.1178
5.08	0.4173	216.3283	5.69	0.4563	236.5459
5.16	0.4225	219.024	5.79	0.4632	240.1229
5.27	0.4302	223.0157	5.94	0.4734	245.4106
5.43	0.4416	228.9254	6.16	0.4884	253.1866
5.67	0.4583	237.5827	6.29	0.4967	257.4893
5.8	0.4674	242.3002	6.47	0.5088	263.7619
5.94	0.4766	247.0694	6.57	0.5156	267.287
6.07	0.4857	251.7869	6.72	0.5255	272.4192
6.27	0.4991	258.7334	6.8	0.5311	275.3222
6.38	0.5066	262.6214	6.93	0.5394	279.625
6.54	0.5176	268.3238	7.11	0.5513	285.7939
6.63	0.5238	271.5379	7.21	0.5581	289.319
6.77	0.5328	276.2035	7.31	0.5648	292.7923
6.85	0.5378	278.7955	7.4	0.5713	296.1619
6.96	0.5454	282.7354	7.55	0.5809	301.1386
7.02	0.5495	284.8608	7.63	0.5863	303.9379
7.08	0.5537	287.0381	7.75	0.5942	308.0333
7.15	0.5578	289.1635	7.81	0.5986	310.3142
7.24	0.5639	292.3258	7.91	0.6049	313.5802
7.38	0.5731	297.095	8	0.6113	316.8979
7.59	0.5866	304.0934	8.1	0.6175	320.112
7.7	0.5942	308.0333	8.19	0.6237	323.3261
7.87	0.6054	313.8394	8.28	0.6295	326.3328
7.97	0.6118	317.1571	8.37	0.6356	329.495
8.11	0.621	321.9264	8.46	0.6416	332.6054
8.31	0.6345	328.9248	8.55	0.6474	335.6122
8.51	0.6476	335.7158	8.68	0.6559	340.0186
8.71	0.6604	342.3514	8.8	0.6644	344.425
8.9	0.6729	348.8314	8.93	0.6728	348.7795
8.95	0.6761	350.4902	9.05	0.6809	352.9786
9	0.6792	352.0973	9.17	0.6891	357.2294
9.07	0.6838	354.4819	9.29	0.6973	361.4803
9.11	0.6864	355.8298	9.41	0.7053	365.6275
9.17	0.6902	357.7997	9.44	0.7075	366.768
9.25	0.6958	360.7027	9.47	0.7095	367.8048
9.34	0.7015	363.6576	9.52	0.7125	369.36
9.43	0.7071	366.5606	9.58	0.7168	371.5891
9.45	0.7086	367.3382	9.65	0.7212	373.8701
9.47	0.71	368.064	9.71	0.7256	376.151
9.5	0.712	369.1008	9.78	0.7299	378.3802

9.53	0.7141	370.1894
9.57	0.7162	371.2781
9.61	0.7192	372.8333
9.68	0.7237	375.1661
9.75	0.7283	377.5507
9.82	0.7328	379.8835
9.89	0.7373	382.2163
9.96	0.7417	384.4973
10	0.7462	386.8301
10.1	0.7506	389.111
10.2	0.7566	392.2214
10.4	0.7655	396.8352
10.5	0.7744	401.449
10.7	0.7831	405.959
10.8	0.7916	410.3654
11	0.8001	414.7718
11.1	0.8086	419.1782
11.3	0.8168	423.4291
11.5	0.8246	427.4726
11.6	0.8322	431.4125
540 mm eccentricity		
Deflection	load factor	load
0	0	0
0.572	5.00E-02	25.91896
1.14	9.99E-02	51.80734
2.01	0.1741	90.25344
3.14	0.2675	138.672
3.42	0.2893	149.9731
3.58	0.3013	156.1939
3.81	0.319	165.3696
4.16	0.3447	178.6925
4.35	0.3587	185.9501
4.63	0.3784	196.1626
4.78	0.3892	201.7613
4.86	0.3952	204.8717
4.99	0.404	209.4336
5.06	0.4089	211.9738
5.17	0.4161	215.7062
5.32	0.4268	221.2531
5.41	0.4328	224.3635
5.53	0.4414	228.8218
5.6	0.4462	231.3101
5.7	0.4532	234.9389
5.76	0.4572	237.0125
5.85	0.463	240.0192
5.89	0.4662	241.6781
5.96	0.471	244.1664
6.07	0.4782	247.8989
6.13	0.4821	249.9206

6.21	0.4879	252.9274
6.34	0.4966	257.4374
6.41	0.5013	259.8739
6.51	0.5084	263.5546
6.57	0.5124	265.6282
6.66	0.5181	268.583
6.78	0.5266	272.9894
6.85	0.5312	275.3741
6.95	0.5381	278.951
7.01	0.542	280.9728
7.09	0.5475	283.824
7.13	0.5507	285.4829
7.2	0.5553	287.8675
7.25	0.5584	289.4746

References

Ansourian, P. (1981). "Experiments on continuous composite beams" *Proc. Instn Civ. Engrs*, Part 2 1981;71 25-51.

Baskar, K., Shanmugam, N.E., and Thevendran, V. (2002). "Finite-element analysis of steel-concrete composite plate girder." *J. Struct. Eng.*, 128(9), 1158-1168.

Baskar, K., Shanmugam, N.E. (2003). "Steel-concrete composite plate girders subject to combined shear and bending" *J. Constr. Steel Res.*, 59: 531-557.

Chapman, J.C., and Balakrishnan, S. (1964). "Experiments on Composite Beams." *Struct. Eng.*, 42(11), 369-383.

Ghosh, B., and Mallick, S.K. (1979). "Strength of steel-concrete composite beams under combined flexure and torsion." *The Indian Concrete Journal*, 53, 48-53.

Hirst, M.J.S., Yeo, M.F. (1980). "The analysis of composite beams using standard finite element programs." *Comput. Struct.*, 11(3), 233-237.

Liang, Q.Q., Uy, B., Bradford, M.A., Ronagh, H.R. (2005), "Strength Analysis of Steel-Concrete Composite Beams in Combined Bending and Shear." *J. Struct. Eng.*, ASCE, 131(10), 1593-1600.

Liang, Q.Q., Uy, B., Bradford, M.A., Ronagh, H.R. (2004). "Ultimate strength of continuous composite beams in combined bending and shear." *J. Constr. Steel Res.*, 60(8), 1109-1128.

Ray, M.B., and Mallick, S.K. (1980). "Interaction of flexure and torsion in steel-concrete composite beams." *The Indian Concrete Journal*, 54, 80-83.

Razaqpur, A.G., Nofal, M. (1990). "Analytical modeling of nonlinear behaviour of composite bridges." *J. Struct. Eng.*, ASCE, 116(6), 1715-1733.

Razaqpur, A.G., Nofal, M. (1989). "A finite element for modelling the nonlinear behaviour of shear connectors in composite structures." *Comput. Struct.*, 32(1), 169-174.

Standards Australia (2003). "Composite Structures, part I: Simply supported beams." *AS 2327.1*, Sydney.

Sebastian, W., and McConnel, R.E. (2000). "Nonlinear FE Analysis of Steel-Concrete Composite Structures." *J. Struct. Eng.*, 126(6), 662-674.

Singh, R.K., and Mallick, S.K. (1977). "Experiments on steel-concrete composite beams subjected to torsion and combined flexure and torsion." *The Indian Concrete Journal*, 51, 24-30.

Thevendran, V., Chen, S., Shanmugam, N.E., and Liew, J.Y.R. (1999).

“Nonlinear analysis of steel-concrete composite beams curved in plan.” *Finite Elem. Anal. Design*, 32(3), 125-139.

Yam, L.C.P., Chapman, J.C. (1968) “The inelastic behaviour of continuous composite beams of steel and concrete” *Proc. Inst. Civ. Eng. Part 2*, 53, 487-501.

Yam, L.C.P., Chapman, J.C. (1968) “The inelastic behaviour of simply supported composite beams of steel and concrete.” *Proc. Inst. Civ. Eng.*, 41(1), 651-683.